NATIONAL ADVISORY COMMITTEE FOR AERONAUTICS

TECHNICAL NOTE 3770

IMPINGEMENT OF DROPLETS IN 60° ELBOWS WITH POTENTIAL FLOW

By Paul T. Hacker, Paul G. Saper, and Charles F. Kadow

Lewis Flight Propulsion Laboratory
Cleveland, Ohio

Washington
October 1956

NATIONAL ADVISORY COMMITTEE FOR AERONAUTICS

TECHNICAL NOTE 3770

IMPINGEMENT OF DROPLETS IN 60° ELBOWS WITH POTENTIAL FLOW

By Paul T. Hacker, Paul G. Saper, and Charles F. Kadow

SUMMARY

Trajectories were determined for water droplets or other aerosol particles in air flowing through 60° elbows especially designed for two-dimensional potential motion. The elbows were established by selecting as walls of each elbow two streamlines of a flow field produced by a complex potential function that establishes a two-dimensional flow around a 60° bend. An unlimited number of elbows with slightly different shapes can be established by selecting different pairs of streamlines as walls. Some of these have a pocket on the outside wall. The elbows produced by the complex potential function are suitable for use in aircraft air-inlet ducts and have the following characteristics:

(1) The resultant velocity at any point inside the elbow is always greater than zero but never exceeds the velocity at the entrance.

(2) The air flow field at the entrance and exit is almost uniform and rectilinear.

(3) The elbows are symmetrical with respect to the bisector of the angle of bend.

These elbows should have lower pressure losses than bends of constant cross-sectional area.

The droplet impingement data derived from the trajectories are presented along with equations so that collection efficiency, area, rate, and distribution of droplet impingement can be determined for any elbow defined by any pair of streamlines within a portion of the flow field established by the complex potential function. Coordinates for some typical streamlines of the flow field and velocity components for several points along these streamlines are presented in tabular form. A comparison of the 60° elbow with previous calculations for a comparable 90° elbow indicated that the impingement characteristics of the two elbows were very similar.

INTRODUCTION

As part of a comprehensive research program concerning the problem of ice protection of aircraft, an investigation of the impingement of cloud droplets on airfoils, aerodynamic bodies, and other aircraft components has been undertaken by the NACA Lewis laboratory. The investigation includes theoretical calculations of cloud droplet impingement on airfoils, cylinders, spheres, ellipsoids of revolution, air inlets, and 90° elbows (refs. 1 to 12). These calculations were made with the aid of differential analyzers developed at the NACA Lewis laboratory.

In furtherance of this research program this report presents droplet impingement calculations for a 60° elbow with potential flow. This 60° elbow is similar to the 90° elbow of reference 12 in that the elbow design was obtained from the same generalized complex potential function. In this study more of the flow field established by the complex potential function was used than for the 90° elbow in order to obtain an elbow with a pocket on the outside wall. This pocket was included in the study to determine the effect of such configurations on collection efficiencies and distribution of impinging water. The water-droplet impingement data as well as the elbow and flow field are presented in dimensionless form in order to make the results applicable for a wide range of meteorological and flight conditions, as well as for sizes and shapes of elbows. The impingement data presented herein are not restricted to supercooled water droplets, but may be applied to other aerosol particles as long as the drag coefficient of the particles is comparable to spheres of the same mass.

ANALYSIS

Equations of Droplet Motion

As an airfoil or aircraft component moves through a cloud, the interception of cloud droplets by the object is dependent on the physical configuration of the component, the flight conditions, and the inertia of the cloud droplets. In order to obtain the extent of impingement and the rate of droplet impingement per unit area on the component, the cloud-droplet trajectories with respect to the component must be determined. The differential equations that describe the droplet motion in a two-dimensional flow field are derived in reference 4 and are presented herein in the following form:

$$\left.\begin{aligned} \frac{dv_x}{d\tau} &= \frac{C_D Re}{24}\frac{1}{K}(u_x - v_x) \\ \frac{dv_y}{d\tau} &= \frac{C_D Re}{24}\frac{1}{K}(u_y - v_y) \end{aligned}\right\} \tag{1}$$

where

$$K = \frac{2}{9}\frac{\rho_w a^2 U}{\mu l} \tag{2}$$

(with U in ft/sec), and the Reynolds number Re is obtained in terms of the free-stream Reynolds number

$$Re_0 = \frac{2a\rho_a U}{\mu} \tag{3}$$

(U in ft/sec) so that

$$\left(\frac{Re}{Re_0}\right)^2 = (u_x - v_x)^2 + (u_y - v_y)^2 \tag{4}$$

(All symbols are defined in appendix A.)

Values of coefficient of drag for water droplets C_D used in calculations are those presented in reference 13 for solid spheres. In accordance with these equations, the droplet trajectories with respect to an elbow depend on radius of the droplets, air speed, density of water or aerosol particle, air density, and air viscosity as first-order variables. The trajectories also depend on the size and geometric configuration of the elbow, since these determine the magnitude of the component velocities u_x and u_y of the air everywhere in the flow field inside the elbow.

Elbow Geometry and Flow Field

As in the case of the 90° elbow of reference 12, the air-flow field for the elbow studied in this report was not determined for a given elbow, but was determined by establishing from potential theory a two-dimensional flow field that makes a 60° turn. From this flow field two streamlines were selected as walls of the elbow. Selection of the complex potential function and streamlines as walls was based upon the following criteria:

(1) The air-flow field should be uniform and rectilinear at some point before and after the bend, in order that the elbow may be fitted to straight ducts.

(2) The resultant velocity at any point inside the elbow should not exceed the velocity U where the flow is uniform and rectilinear. This criterion was selected so as to minimize possible flow separation.

(3) No streamline should have singular points (0 or ∞ velocity) within the elbow.

A complex potential function that establishes a flow field, a portion of which nearly satisfies all the criteria of the preceeding paragraph for an elbow, is given in generalized form by

$$e^{\left(\frac{ie^{-i\delta/2}}{\sin \delta/2}\right)\frac{\zeta}{l}} = e^{\left(\frac{ie^{-i\delta/2}}{\sin \delta/2}\right)\frac{\omega}{lU}} + e^{\left(\frac{ie^{i\delta/2}}{\sin \delta/2}\right)\frac{\omega}{lU}} \tag{5}$$

where δ is the angle of bend of the elbow, in this case 60°. This equation is identical to the complex potential function that was used to establish the 90° elbow of reference 12. The use of this complex potential function to design elbows is discussed in references 14 and 15. Details (required for this impingement study) for designing a 60° elbow and determining its velocity field and other physical characteristics from equation (5) are given in appendix B.

A portion of the streamline pattern given by equation (5) is shown in figure 1. The flow field between the two streamlines $\psi = 15\pi lU/32$ and $\psi = \pi lU/12$ satisfies all the assumed criteria for a 60° elbow. The first condition is strictly fulfilled only at infinity, but the flow approaches uniform and rectilinear motion very rapidly before and after the bend. Therefore, the ends of the elbow may be selected at some reasonable distance before and after the bend without serious error (see appendix B). For this droplet impingement study, the ends of the elbow are defined by the lines $\eta = 0.5774\xi - 0.866\pi l$ and $\xi = \frac{3}{4}\pi l$, indicated by dashed lines in figure 1. These ends are comparable to those of the 90° elbow of reference 12 in that they are the same distance $\frac{3}{4}\pi l$ measured in the direction of flow from the origin of the coordinate system.

Since the flow field between the streamlines $\psi = \pi lU/12$ and $\psi = 15\pi lU/32$ satisfies the assumed criteria, any pair of streamlines between these two may be selected as walls of a two-dimensional elbow. However, elbows defined by pairs of streamlines between $\psi = \pi lU/12$ and $\psi = 4\pi lU/12$ are probably the most practical elbows, because they more nearly approximate conventional elbows. Of all the possible elbows defined by pairs of streamlines between $\psi = \pi lU/12$ and $\psi = 4\pi lU/12$, the most useful elbow is probably the elbow defined by these two streamlines because for a given entrance width the average turning radius is smaller for this elbow than for any elbow defined by a pair of streamlines between these two. (Definition of turning radius and elbow entrance width and their relation to the linear parameter l of eq. (5) are given

in appendix B.) For this droplet impingement study the streamline pattern of figure 1 is divided into three classes of elbows:

(1) The elbow defined by streamlines $\psi = \pi l U/12$ and $\psi = 4\pi l U/12$ is defined as the basic elbow.

(2) Elbows defined by any pair of streamlines between those of the basic elbow or by one streamline of the basic elbow and any other intermediate streamline are designated as supplementary elbows.

(3) Elbows whose outside wall is defined by the streamline $\psi = 15\pi l U/32$ are designated as pocket elbows.

The entrance width and average turning radius for the basic elbows are approximately equal to $\frac{\pi l}{4}$ and $\frac{3}{4}\pi l \cot 30^\circ + \frac{5\pi l}{24}$ (less than 1 percent error), respectively (fig. 1 and appendix B), with center of turning located at $\xi = \frac{3}{4}\pi l$ and $\eta = -\frac{3}{4}\pi l \cot 30^\circ$ (point A fig. 1). The entrance width and turning radii for supplementary and pocket elbows may be approximated by equations given in appendix B.

In order to calculate conveniently the droplet impingement data for an elbow over a large range of conditions as well as elbow size, it is necessary to express the elbow and its velocity field in terms of dimensionless parameters. This end is accomplished by expressing all distances relative to an elbow as ratios to the linear parameter l and all velocities as ratios to the free-stream velocity U. The method of obtaining the elbow and velocity field from equation (5) in terms of dimensionless parameters is presented in appendix B. The basic elbow with some intermediate streamlines (supplementary elbows) and the pocket elbow are shown in figure 2 in terms of dimensionless parameters x and y. Figure 2, with the elbow entirely in the first quadrant, was obtained from figure 1 by the following transformation equations: $x = 0.866\xi - 0.5\eta + 2.00$ and $y = 0.5\xi + 0.866\eta + 3.00$. (The transformation was made in order to facilitate droplet-trajectory calculations with the electromechanical differential analyzer.) Also shown in figure 2 are some typical droplet trajectories and lines of constant distance from the elbow entrance.

The velocity field for the entire streamline pattern of figure 2 is presented in figure 3 in terms of dimensionless parameters. In figure 3(a), the x-component of velocity u_x is given as a function of x for constant values of y, and in figure 3(b), the y-component of velocity u_y is given as a function of y for constant values of x. The component velocities u_x and u_y are dimensionless and are equal to the ratio of the actual component velocity to the free-stream velocity U. Streamline coordinates and velocity components as a function of velocity potential are tabulated in table I.

An elbow designed by the use of equation (5) may have any entrance cross-sectional configuration. The only conditions that must be satisfied are (1) the streamlines that form the wall of the elbow at the entrance must remain on the walls throughout the elbow, and (2) the streamlines that form the walls of the elbow are identical to or lie within the streamlines $\psi = \pi l U/12$ and $\psi = 15\pi l U/32$ if the assumed criteria for an elbow are to be fulfilled. An elbow with a rectangular entrance cross section is the most convenient elbow with respect to construction and application of droplet-trajectory data in determining area, rate, and distribution of water droplet impingement. Therefore, the droplet impingement data presented in the RESULTS AND DISCUSSION apply directly to elbows with rectangular entrance cross section. However, the same droplet impingement data may be used to find area, rate, and distribution of water droplet impingement for elbows with any entrance cross section. A method for applying the results to nonrectangular entrance cross sections is outlined in appendix C of reference 12.

METHOD OF SOLUTION

The differential equations of motion of a droplet in a two-dimensional flow field are difficult to solve by ordinary means, because the values of the component relative velocities between air and droplet required to solve equation (1) are functions of the droplet position and velocity, and these are not known until the trajectory is traced. The total relative velocity at each position is also required in order to determine the value of the local Reynolds number Re (eq. (4)). Simultaneous solutions for the two equations were obtained with an electromechanical differential analyzer constructed at the Lewis laboratory. The results from the differential analyzer were in the form of plots of droplet trajectories with respect to the elbow.

The equations of motion (eq. (1)) were solved for the following values of the inertia parameter K: 1/3, 4/7, 1, 2, 4, and 8. For each value of K, a series of trajectories was computed for each of these four values of free-stream Reynolds number Re_0: 0, 32, 128, and 512. The end of the elbow nearer the origin of figure 2 was chosen as the entrance. Trajectories were computed for the various combinations of K and Re_0 for droplets that entered the elbow at several positions across the entrance.

Assumptions necessary to the solution of the problem are:

(1) The droplets enter the elbow with the same velocity as the air, which is approximately free-stream (fig. 3).

(2) The droplets are always spherical and do not change size.

(3) No gravitational force acts on the droplets.

RESULTS AND DISCUSSION

Method of Presenting Data

The impingement data presented in this section, which apply only to elbows with rectangular entrance cross sections, are divided into three categories: (1) those for the basic elbow (defined by the streamlines $\psi = \pi\ell U/12$ and $4\pi\ell U/12$), (2) those for supplementary elbows (defined by a pair of streamlines between those for the basic elbow or one streamline of the basic elbow and any other intermediate streamline), and (3) those for pocket elbows (elbows which have $\psi = 15\pi\ell U/32$ as a wall).

For convenience in presenting and discussing the impingement results, the wall with the largest value of ψ is designated as the outside wall, and the other as the inside wall. Because of the physical configurations of the elbow (flow field) and the direction of droplet inertia forces, droplet impingement can occur only on the outside wall of the elbow. The area of impingement on the outside wall of the basic and supplementary elbow starts at the entrance and extends in a downstream direction, the extent depending upon the values of K and Re_0. The area of impingement for pocket elbows, however, does not start at the entrance but at some point downstream depending upon the values of K and Re_0.

In presenting the data, use is made of the abscissa values of streamlines and droplet trajectories at the elbow entrance. In order to differentiate between abscissa values for streamlines and droplet trajectories, the notation adopted herein (illustrated in fig. 4) involves the use of double subscripts for the x-coordinate. The first subscript of each pair indicates that the abscissa value refers to a streamline ψ or to a droplet trajectory d. The second subscript refers to a particular streamline or droplet trajectory; for example, o refers to the outside wall, and m refers to the maximum initial value of abscissa of droplets that impinge in the elbow. Symbols having a prime superscript refer to the basic elbow, unprimed symbols to supplementary elbows, and symbols with an asterisk superscript refer to a pocket elbow.

An analysis of the series of droplet trajectories computed for the elbow showed that all the important information necessary to calculate collection efficiency, extent of impingement, rate, and distribution of droplet impingement could be summarized in terms of

(1) Entrance width of elbow being considered

(2) Distance along outside wall from entrance of elbow to point at which droplet trajectory meets the outside wall. (Distance is denoted as S' for basic elbow and is dimensionless with same dimensionless scale as x. Some lines of constant S are shown in fig. 2 along with some typical streamlines.)

(3) Abscissa value of droplet trajectories at elbow entrance (x_d' for basic elbow)

(4) Values of dimensionless parameters K and Re_0

Presentation of impingement data in terms of the dimensionless parameters K and Re_0 is very convenient, but the physical significance of the parameters is often obscure unless use is made of their definitions (eqs. (2) and (3)). In order that these dimensionless parameters have some physical significance in the following discussion, some typical combinations of K and Re_0 are presented in table II in terms of elbow size, droplet size, free-stream velocity, air density, and air viscosity.

Basic Elbow

The droplet trajectory information required to calculate the maximum extent of impingement, the collection efficiency, the rate of impingement, and the distribution of impingement for the basic elbow is summarized for various combinations of K and Re_0 in figure 5. This figure is a plot of the distance S' along the outside wall of the elbow from the entrance to the point of impingement of droplets that enter the elbow at various values of x_d'. (The length of the outside wall of the basic elbow is 5.68.) The data presented in figure 5(a) for $Re_0 = 0$ (Stokes' law) can be considered as a limiting case, since they apply to an ideal situation that cannot be attained in practice. The curves for $K = \infty$ represent a limiting case in which the conditions are such that the droplet trajectories are straight lines parallel to the direction of the free-stream velocity U.

Maximum extent of impingement. - The maximum extent of impingement for the basic elbow S_m' for a given combination of K and Re_0 is determined from figure 5 by the maximum value of S' for any value of x_d' within the walls of the elbow. For some combinations of K and Re_0 such as $K = 1$ and $Re_0 = 32$ (fig. 5(b)), impingement occurs throughout the entire length of the elbow with some droplets passing through without impinging, as is illustrated in figure 4(a). For other combinations of K and Re_0, such as $K = 4$ and $Re_0 = 128$ (fig. 5(c)), the impingement of all droplets is confined to a portion of the outside wall, as is

illustrated in figure 4(b). The maximum extent of impingement when $K = 4$ and $Re_0 = 512$ (fig. 5(d)) is 5.31. The maximum extent of impingement S'_m is presented in figure 6 as a function of the reciprocal of K for four values of Re_0 and in table II for some typical values of K and Re_0. The value of S'_m varies directly with Re_0 and inversely with K.

Droplet trajectories were computed beyond the exit of the elbow for some combinations of K and Re_0. These extended trajectories were computed for a uniform rectilinear flow field with velocity U such as would be present in a straight duct connected to the elbow. The trajectories of the droplets before emerging at the exit of the elbow were almost parallel to the air streamline at the exit (fig. 2), and upon entering the uniform flow field of the straight duct the droplet trajectories became so nearly parallel to the streamlines and outside wall that it was difficult to determine the exact point of impingement. Because of this difficulty, the data on maximum extent of impingement presented in figures 5 and 6 are terminated at the exit of the basic elbow ($S' = 5.68$). Although there is some impingement in the straight duct, the amount of water impinging per unit area is small, as is discussed in a later section.

Collection efficiency. - Collection efficiency E' of the elbow is defined as the ratio of the amount of water impinging within the elbow to the amount of water entering the elbow. If the assumption is made that the water droplets are uniformly dispersed in the air entering the elbow, then the collection efficiency can be expressed in terms of the width of the elbow at the entrance $x'_{\psi,i} - x'_{\psi,o}$ and the difference in abscissa values at the elbow entrance of the two droplet trajectories that define the extent of impingement. The abscissa value of the trajectory that defines the forward boundary of impingement ($S' = 0$), defined as $x'_{d,o}$, has the same value as the outside wall of the elbow $x'_{\psi,o}$ (fig. 4). The abscissa value of the trajectories that define the rearward extent of impingement, designated as $x'_{d,m}$ (fig. 4), is determined from figure 5 at the maximum value of S' for a given combination of values of K and Re_0. The difference $x'_{d,m} - x'_{d,o}$ is proportional to the amount of water impinging on the elbow wall, and the width of the elbow entrance $x'_{\psi,i} - x'_{\psi,o}$ is proportional to the total amount of water in droplet form entering the elbow. Hence, the collection efficiency E' is given by

$$E' = \frac{x'_{d,m} - x'_{d,o}}{x'_{\psi,i} - x'_{\psi,o}} \tag{7}$$

For the basic elbow, $x'_{\psi,i} - x'_{\psi,o} = 0.7900$ (appendix B), and equation (7) becomes

$$E' = \frac{x'_{d,m} - x'_{d,o}}{0.7900} \tag{8}$$

Values of $x'_{d,m} - x'_{d,o}$ as a function of K for four values of Re_0 are plotted in figure 7.

The collection efficiency of the basic elbow, obtained by equation (8) and the data of figure 7, is presented in figure 8 as a function of K for four values of Re_0 and in table II for some typical values of K and Re_0. For a given value of Re_0, the collection efficiency increases with increasing K until all the droplets entering the elbow impinge upon the outside wall. The value of K for which the collection efficiency is unity increases with increasing value of Re_0.

Rate of water interception. - The total rate of water interception W'_m is defined for the elbow as the amount of water intercepted per unit time by a unit depth of elbow. Depth is measured in a direction perpendicular to the plane of flow (perpendicular to plane of fig. 2). The total rate of water interception is determined by the spacing of the two trajectories that define the extent of impingement $(x'_{d,m} - x'_{d,o})$, the liquid-water content w, and the free-stream velocity U. For the basic elbow the total rate of water interception can be calculated from the information in figure 7 and the following relation:

$$W'_m = 0.33\,(x'_{d,m} - x'_{d,o})\ell U w \tag{9}$$

where U is in miles per hour and w is in grams per cubic meter. The total rate of water interception can also be determined from the collection efficiency E' (fig. 8) and the following relation:

$$W'_m = 0.33\,E'(x'_{\psi,i} - x'_{\psi,o})\ell U w \tag{10}$$

where $x'_{\psi,i} - x'_{\psi,o}$ is the width of the basic elbow entrance. Since $x'_{\psi,i} - x'_{\psi,o} = 0.79$ for the basic elbow, equation (10) reduces to

$$W'_m = 0.261\,E'\ell U w \tag{11}$$

The linear parameter ℓ appears in equations (9), (10), and (11) in order that W'_m have dimensions, and the depth in these equations is measured in feet.

Local rate of droplet impingement. - A knowledge of the local rate of droplet impingement W'_β is required in the design of certain types of thermal anti-icing systems. This rate, which is defined as the amount of water impinging per unit time per unit area of elbow surface, can be determined by the following expression:

$$W'_\beta = 0.33\ Uw \frac{dx'_d}{dS'} = 0.33\ Uw\beta' \tag{12}$$

(where U is in mph). The quantity 0.33 Uw of equation (12) is the amount of water entering the elbow per unit time per unit area, and β' is the local impingement efficiency dx'_d/dS'. The values of β' as a function of S' for various combinations of K and Re_0 are presented in figure 9. The values of β' were obtained by graphically determining the reciprocals of the slopes of the curves presented in figure 5. The curves of figure 9 show that the maximum value of β', and therefore the maximum local rate of droplet impingement W'_β, occurs between $S' = 2.75$ and $S' = 4$ for all combinations of values of K and Re_0 studied.

The dashed lines in figure 9 are the limits in S of the impingement area, and β' is zero for any combination of K, Re_0, and S that falls beyond this limit. For some combinations of K and Re_0 (e.g., $K = 1$, $Re_0 = 128$, fig. 9(c)), the β' curves do not meet this limit within the elbow ($S = 5.68$). In these cases, impingement occurs throughout the entire length of the elbow and may extend into a straight duct attached to the exit. The value of β' and the maximum extent of impingement in the straight duct can be estimated by extrapolating the curves of figure 9 beyond $S = 5.68$ until $\beta' = 0$. The largest value that β' may have at the exit of the elbow for any combination of values of K and Re_0 is determined by the dashed line and is approximately 0.09. Thus, for any point beyond the exit on the wall of a straight duct the values of β' are less than 0.09.

Supplementary Elbows

In some applications, supplementary elbows, which may be derived from the flow field of the basic elbow by selecting any pair of streamlines as walls, may be more desirable than the basic elbow. Therefore, droplet impingement data for them are desirable. Such data may be determined from the series of droplet trajectories calculated for the various combinations of K and Re_0 for the basic elbow. However, the presentation of the impingement characteristics for all possible supplementary elbows in the same manner as for the basic elbow is impractical

because of the limitless number of elbows possible. Analysis of the impingement data for supplementary 60° elbows shows that the relations that were valid along lines of constant S for the 90° elbow of reference 12 were also valid for the 60° elbows. Therefore, all the important characteristics required to calculate the extent, rate, and distribution of impingement for any supplementary 60° elbow can be determined from those of the basic 60° elbow by equations that contain empirically determined coefficients. These empirical equations are similar in form to those used for the 90° elbows of reference 12. In these equations, $x_{\psi,o}$, which is determined by the streamline chosen for the outside wall, is an independent variable. A supplementary elbow may be formed from the basic elbow by choosing other streamlines for either the outside wall or the inside wall or both. The empirical equations are, however, either independent of the inside wall $x_{\psi,i}$ or depend on it only in the form $x_{\psi,i} - x_{\psi,o}$, the entrance width. The value of $x_{\psi,i}$ does, nevertheless, establish a limit to the range within which the equations are valid for the elbow chosen.

Maximum extent of impingement. - Curves of S as a function of x_d, similar to those of figure 5 for the basic elbow, can be obtained for any supplementary elbow by the following empirical equation:

$$(x_d)_S = \alpha(x_{\psi,o} - 0.9528) + (x_d')_S \qquad (13)$$

where

$(x_d)_S$ abscissa at elbow entrance of droplets impinging on outside wall of supplementary elbow at distance S from entrance

$(x_d')_S$ abscissa at elbow entrance of droplets impinging on outside wall of basic elbow at distance S from entrance (fig. 5)

$(\ )_S$ denotes that the value of S is the same for x_d and x_d'

α empirical coefficient, function of S, K, and Re_0 (fig. 10)

$x_{\psi,o}$ abscissa at elbow entrance of streamline designated as outside wall of supplementary elbow

0.9528 constant, abscissa at entrance of outside wall of basic elbow

The values of K and Re_0 that apply to $(x_d)_S$ are the same as those for $(x_d')_S$. For some combinations of S, K, and Re_0, equation (13) gives values of x_d larger than $x_{\psi,i}$, the inside wall of a supplementary elbow. In this case, all droplets that enter the elbow impinge

upon the outside wall. As an example of the use of equation (13), assume that it is desired to find x_d of a droplet that impinges at $S = 2.5$ on the streamline $\psi = 9\pi\ell U/32$ ($x_{\psi,o} = 1.1179$), which is designated as the outside wall, for $K = 1$ and $Re_0 = 32$. From figure 5(b) at $S = 2.5$, $x_d' = 1.031$, and from figure 10(b), $\alpha = 1.241$. Substitution of these values into equation (13) gives

$$(x_d)_{2.5} = 1.241\ (1.1179 - 0.9528) + 1.031 = 1.236$$

The range over which values of S may be selected depends upon the particular streamline designated as the outside wall of the supplementary elbow (see fig. 2). The range of S as a function of $x_{\psi,o}$ is presented in figure 11. After the curves of S as a function of x_d are established for a particular supplementary elbow, the maximum extent of impingement S_m is found in the same manner as for the basic elbow.

Collection efficiency. - The collection efficiency E for any supplementary elbow can be calculated from the curves of S as a function of x_d as determined in the preceeding section by the following equation:

$$E = \frac{x_{d,m} - x_{d,o}}{x_{\psi,i} - x_{\psi,o}} \tag{14}$$

which is similar to equation (7) for the basic elbow. However, analysis of the impingement data for supplementary elbows showed that the collection efficiency for any supplementary elbow could be determined from the collection efficiency E' for the basic elbow by the following empirical equation

$$E = \frac{E'(x_{\psi,i}' - x_{\psi,o}') + \gamma(x_{\psi,o} - x_{\psi,o}')}{x_{\psi,i} - x_{\psi,o}} \tag{15}$$

where

E' collection efficiency of basic elbow for given combination of K and Re_0

$x_{\psi,i}' - x_{\psi,o}'$ entrance width of basic elbow, equal to 0.79

γ empirical coefficient, function of K and Re_0 (fig. 12)

$x_{\psi,o} - x_{\psi,o}'$ difference in abscissa of outside walls of supplementary and basic elbow ($x_{\psi,o}' = 0.9528$)

$x_{\psi,i} - x_{\psi,o}$ entrance width of supplementary elbow

Substitution of the appropriate values for the basic elbow in equation (15) gives

$$E = \frac{0.79\ E' + \gamma(x_{\psi,o} - 0.9528)}{x_{\psi,i} - x_{\psi,o}} \tag{16}$$

As an example of the use of equation (16), assume that the collection efficiency for a supplementary elbow defined by $x_{\psi,o} = 1.2$ and $x_{\psi,i} = 1.7$ is desired for $K = 1$ and $Re_o = 128$. From figure 8, $E' = 0.523$ for the basic elbow, and from figure 12, $\gamma = 0.338$. Substitution of these values into equation (16) gives

$$E = \frac{0.79\ (0.523) + 0.338\ (1.2 - 0.9528)}{1.7 - 1.2} = 0.993$$

In some cases the collection efficiency as given by equation (16) is greater than unity. In these cases, all the droplets that enter the elbow impinge upon the outside wall ahead of the exit, and the collection efficiency is assumed unity.

Rate of water interception. - The total rate of water interception per unit depth W_m for a supplementary elbow can be obtained from the following equation, which is identical in form to equation (10) for the basic elbow:

$$W_m = 0.33\ E(x_{\psi,i} - x_{\psi,o})lUw \tag{17}$$

where

E collection efficiency of supplementary elbow (determined by eq. (16))

$x_{\psi,i} - x_{\psi,o}$ entrance width

U free-stream velocity, mph

w liquid-water content, g/cu m

Local rate of droplet impingement. - The local rate of droplet impingement W_β for a supplementary elbow can be determined by

$$W_\beta = 0.33\ Uw\ \frac{dx_d}{dS} = 0.33\ Uw\beta \tag{18}$$

which is identical in form to equation (12) for the basic elbow. The values of the local impingement efficiency β as a function of S may be determined by two methods. Curves of S as a function of x_d are established by equation (13) for a particular supplementary elbow and values of K and Re_0. The reciprocal of the slopes of these curves is equal to β. The second method is based upon the definition of the local impingement efficiency

$$\beta = \frac{dx_d}{dS} \tag{19}$$

Differentiating equation (13) with respect to S gives

$$\beta = \frac{d(x_d)_S}{dS} = \frac{d\alpha}{dS}\left(x_{\psi,o} - 0.9528\right) + \frac{d(x_d')_S}{dS} \tag{20}$$

where

$d\alpha/dS$ derivative of α curves (fig. 10)

$x_{\psi,o}$ abscissa at entrance of outside wall of supplementary elbow

$d(x_d')_S/dS$ equal to β' for basic elbow at given value of S (fig. 9)

Equation (20) may also be written

$$\beta = \frac{d\alpha}{dS}\left(x_{\psi,o} - 0.9528\right) + \beta' \tag{21}$$

Values of $d\alpha/dS$ as a function of S for various values of K and Re_0 are presented in figure 13. These values were determined graphically from the data of figure 10.

The values of K and Re_0 that apply to β are the same as those for β'. As an example of the use of equations (21), assume that β is required at S = 2.5 on the supplementary elbow, the outside wall of which is defined by the streamline $\psi = 9\pi\ell U/32$ ($x_{\psi,o} = 1.1179$), for K = 1 and $Re_0 = 32$. From figure 13(b), $d\alpha/dS = 0.188$ at S = 2.5, and from figure 9(b), $\beta' = 0.148$. Thus,

$$\beta = 0.188\left(1.1179 - 0.9528\right) + 0.148 = 0.179$$

Some caution must be exercised in using equation (18) to calculate local rate of impingement for a supplementary elbow, because values may be obtained that do not apply, depending upon which streamline is selected as the inside wall of the elbow. The inside wall for some values of K

and Re_0 determines the maximum extent of impingement S_m. Therefore, equation (18) should be used in conjunction with the maximum extent of impingement S_m when calculating β or W_β for a particular supplementary elbow; β and W_β are both zero for distances greater than S_m.

Pocket Elbow

Although there are an infinite number of streamlines between $\psi = 4\pi lU/12$ (outside wall of basic elbow) and $\psi = 15\pi lU/32$ that could be selected as outside walls of the pocket elbow, only one has been selected for this study. The one selected is $\psi = 15\pi lU/32$, because it creates the deepest pocket (fig. 2). The droplet trajectory information required to calculate extent, rate, and distribution of droplet impingement for the pocket elbow is summarized for various combinations of K and Re_0 in figure 14. This figure is a plot of the distance S^* along the outside wall of the elbow from the entrance to the point of impingement of droplets that enter the elbow at various values of x_d^*. The length of the outside wall of the pocket elbow is 6.92.

Because of the shape of the pocket elbow, the forward limit of droplet impingement on the outside wall does not start at $S^* = 0$ as it does for the basic and supplementary elbows, but at some distance downstream depending upon the values of K and Re_0. For the following combinations of K and Re_0 there is no impingement on the outside wall of the elbow: $K = 1/3$, $Re_0 = 0$; $K = 1/3$, $Re_0 = 32$; $K = 1/3$, $Re_0 = 128$; and $K = 1/3$, $4/7$, $Re_0 = 512$. For other combinations of K and Re_0, trajectories of droplets that enter the pocket elbow at $x_d^* = 0.5239$ (entrance abscissa of outside wall) are tangent to the outside wall with all other trajectories missing. These values of K and Re_0 are: $K = 4/7$, $Re_0 = 0$; $K = 4/7$, $Re_0 = 32$; $K = 4/7$, $Re_0 = 128$; and $K = 1$, $Re_0 = 512$. These tangent points are indicated by a single point in figure 14.

Maximum extent of impingement. - The maximum extent of impingement for the pocket elbow S_m^* can be determined from figure 14. The maximum extent of impingement depends on three factors: (1) the end of the curves of S_d^* as a function of x_d^*, (2) the choice of inside wall $x_{\psi,i}^*$, and (3) the elbow exit ($S^* = 6.92$).

Collection efficiency. - Collection efficiency of pocket elbows is given by

$$E^* = \frac{x_{d,m}^* - x_{d,o}^*}{x_{\psi,i}^* - x_{\psi,o}^*}$$

where $x^*_{d,m} - x^*_{d,o}$ is difference in abscissa at the entrance of droplet trajectories defining the area of impingement, and $x^*_{\psi,i} - x^*_{\psi,o}$ is the entrance width. A plot of $x^*_{d,m} - x^*_{d,o}$ as a function of K and Re_0 is presented as figure 15. The entrance width of a pocket elbow can have any value up to 1.2189, which is defined by streamlines $\psi = 15\pi lU/32$ and $\psi = \pi lU/12$. Collection efficiencies of two types of pocket elbows are presented in table III. Type A has an entrance width of 0.79 which is the same width as the basic 60° elbow, and type B has an entrance width of 1.2189. Also presented in table III are values of collection efficiencies for the basic 60° elbow. For the same values of K and Re_0, the collection efficiencies of pocket elbows are less than for the basic elbow, with type B elbows having the lowest collection efficiency.

Rate of water interception and local rate of droplet impingement. - The local rate of water interception W^*_m for pocket elbows can be obtained by substitution of appropriate values for pocket elbows into equations (9) or (10) for the basic elbow. The local rate of droplet impingement W^*_β for pocket elbows is obtained by equation (12) with the substitution of β^* the local impingement efficiency of pocket elbows for β'. Plots of β^* for pocket elbows as a function of S^*, K, and Re_0 are presented in figure 16. A comparison of figure 16 with figure 9 shows that local impingement efficiencies for pocket elbows are generally higher than for the basic elbow, although E^* is lower.

COMPARISON OF IMPINGEMENT DATA FOR 60° AND 90° BASIC ELBOWS

A comparison of the collection efficiency of the basic elbow of this report with the basic 90° elbow of reference 12 showed that the collection efficiency of the 60° elbow is slightly higher than that of the 90° elbow at low values of K for all values of Re_0. For high values of K the reverse is true. The collection efficiencies of the basic elbows are summarized in table III. A comparison of the local impingement efficiencies for the 90° and 60° basic elbows at various combinations of values of S, K, and Re_0 showed that the two elbows were very comparable, with the 90° elbow having slightly higher local impingement efficiency values than the 60° elbow at some conditions and slightly lower values for other conditions. This small difference in collection efficiencies and local impingement efficiencies between 60° and 90° elbows would have been difficult to predict before the trajectory calculations for the 60° elbow were made, since the impingement in a straight duct would be zero, and thus it would be assumed that the collection efficiency of a 60° elbow would be less than that for a 90° elbow.

IMPINGEMENT IN CLOUDS OF NONUNIFORM DROPLET SIZE

The impingement data and equations presented in the preceding sections, by which the extent, rate, and distribution of droplet impingement can be determined for the basic, supplementary, and pocket elbows, apply directly to clouds composed of droplets of uniform size. Clouds, however, are not necessarily composed of droplets of uniform size but may have a large range of droplet size. For clouds composed of droplets of nonuniform size, the maximum extent of impingement for elbows is determined by the smallest droplet size present in the cloud. (This is in contrast to the situation involving external aerodynamics or flow around a wing or other body, where the largest droplet determines the maximum extent of impingement.) In order to determine the total and local rates of droplet impingement by equations (10) or (17) and (12) or (18), respectively, for clouds composed of droplets of nonuniform size, the collection efficiency and the local impingement efficiency must be modified. These modified values can be obtained for a given droplet-size distribution pattern by weighting the values of these two quantities for a given size according to the amount of liquid water contained in a given droplet size. A detailed procedure for determining a weighted collection efficiency and local impingement efficiency for a given droplet-size distribution pattern is presented in reference 16.

CONCLUDING REMARKS

The 60° elbows for which droplet impingement data are presented in this report are suitable for aircraft air-inlet ducts and would probably have lower pressure losses than bends with constant cross-sectional areas. However, these impingement data are based upon theoretical calculations for an ideal fluid flow and hence there might be some differences between theoretical and experimental impingement for the same elbow.

Although the collection efficiency of the 60° pocket elbow with the same entrance width as the basic elbow is less than for the 60° basic elbow and the pocket elbow would not be as useful as a droplet inertia separator, the pocket elbow has some impingement characteristics that may be useful. The droplet impingement for pocket elbows is limited to a much smaller area than for the basic elbow; therefore, less area would have to be heated to prevent or remove ice. There is also a region from the entrance to a surface distance of 3.75 on the outside wall of the pocket elbow where there is no impingement. The impingement data for supplementary elbows defined by streamlines near the inside wall of the basic elbow can probably be used to approximate droplet impingement in conventional elbows with long radii of curvature, because the streamlines in this region are approximately equidistant at all points throughout the elbow.

Lewis Flight Propulsion Laboratory
National Advisory Committee for Aeronautics
Cleveland, Ohio, June 19, 1956

APPENDIX A

SYMBOLS

The following symbols are used in this report:

a	droplet radius, ft
C_D	drag coefficient for droplets, dimensionless
d	droplet diameter, microns (3.28×10^{-6} ft)
E	collection efficiency, ratio of amount of water impinging within elbow to amount of water entering elbow, dimensionless
i	imaginary number, $\sqrt{-1}$
K	inertia parameter, $\frac{2}{9}\frac{\rho_w a^2 U}{\mu l}$ where U is in ft/sec, dimensionless
L	width of basic elbow at entrance, $\pi l/4$, ft
l	arbitrary length, proportional to size of elbow, ft
Re	local Reynolds number with respect to droplet, $2a\rho_a\bar{v}/\mu$, dimensionless
Re_0	free-stream Reynolds number with respect to droplet, $2a\rho_a U/\mu$, dimensionless
S	distance along outside wall of elbow, measured from entrance, ratio to l, dimensionless
S_m	maximum extent of impingement, dimensionless
t	time, sec
U	free-stream or entrance velocity, mph or ft/sec as noted
u	local air velocity, ratio to U, dimensionless
v	local droplet velocity, ratio to U, dimensionless
$\bar{v}$	magnitude of local vector difference between droplet and air velocity, ft/sec

W_m rate of water impingement on total elbow surface, per unit depth of elbow, lb/(hr)(ft of depth)

W_β local rate of water impingement on elbow surface, lb/(hr)(sq ft)

w liquid-water content of cloud, g/cu m

x,y rectangular coordinates, ratio to l, dimensionless

x_d abscissa at elbow entrance of any droplet trajectory, dimensionless

$x_{d,m}$ maximum value of abscissa at elbow entrance of droplet trajectory that intersects or is tangent to streamline designated as outside wall of elbow, dimensionless

$x_{d,o}$ minimum value of abscissa at elbow entrance of droplet trajectory (has same value as $x_{\psi,o}$), dimensionless

x_ψ abscissa at elbow entrance of any air streamline inside elbow

$x_{\psi,i}$ abscissa at elbow entrance of streamline designated as inside wall, dimensionless

$x_{\psi,o}$ abscissa at elbow entrance of streamline designated as outside wall, dimensionless

α empirical coefficient (eq. (13)), dimensionless

β local impingement efficiency, dimensionless

γ empirical coefficient (eq. (15)), dimensionless

δ angle of bend of elbow, in this case 60°

ζ complex numbers, $\xi + i\eta$

μ viscosity of air, slugs/(ft)(sec)

ξ,η rectangular coordinates, ft

ρ density, slugs/cu ft

τ time parameter, tU/l, dimensionless

φ velocity potential

ψ stream function

ω complex potential, $\varphi + i\psi$

Subscripts:

a air

S constant distance from elbow entrance

w water

x horizontal component

y vertical component

η vertical component

ξ horizontal component

Superscripts:

' refers to basic elbow defined by streamlines $\psi = 4\pi lU/12$ and $\pi lU/12$

* refers to pocket elbow whose outside wall is $\psi = 15\pi lU/32$

APPENDIX B

SELECTION OF COMPLEX POTENTIAL FUNCTION FOR DESIGN OF 60° ELBOW AND CALCULATION OF FLOW FIELD

Selection of Complex Potential Function

The 60° elbows for which droplet impingement data are presented in the body of the report were designed by selecting as walls of an elbow two streamlines of a two-dimensional incompressible flow field established by a complex potential function. This function, which nearly satisfies all the criteria outlined in the ANALYSIS for a 60° elbow, is discussed in references 14 and 15 and was employed in reference 12 to establish a 90° elbow for which droplet impingement was determined. This complex potential function can be expressed in the following form:

$$e^{\left(\frac{ie^{-i\delta/2}}{\sin \delta/2}\right)\frac{\zeta}{l}} = e^{\left(\frac{ie^{-i\delta/2}}{\sin \delta/2}\right)\frac{\omega}{lU}} + e^{\left(\frac{ie^{i\delta/2}}{\sin \delta/2}\right)\frac{\omega}{lU}} \tag{5}$$

where

i imaginary number, $\sqrt{-1}$

δ angle of bend of elbow, in this case 60°

ζ complex number, $\xi + i\eta$

l arbitrary length, proportional to size of elbow, ft

ω complex potential, $\varphi + i\psi$

U free-stream velocity (constant; velocity at infinity before and after bend)

φ velocity potential

ψ stream function

Calculation of Flow Field

Streamlines. - Parametric equations for the flow streamlines are obtained from equation (5) by separating and equating the real and

imaginary parts of the ζ function to the real and imaginary parts of the ω function. The results of this procedure are:

$$\xi = \frac{l}{\csc^2 \delta/2}\left\{\frac{\varphi}{lU}\cot^2\frac{\delta}{2} - \frac{\psi}{lU}\cot\frac{\delta}{2} + \ln 2 + \ln\sqrt{\cos^2\frac{\psi}{lU} + \sinh^2\frac{\varphi}{lU}} + \cot\frac{\delta}{2}\left[\arctan\left(\tanh\frac{\varphi}{lU}\tan\frac{\psi}{lU}\right)\right]\right\} \tag{B1}$$

and

$$\eta = \frac{l}{\csc^2 \delta/2}\left[\frac{\varphi}{lU}\cot\frac{\delta}{2} + \frac{\psi}{lU}\cot^2\frac{\delta}{2} - \left(\ln 2\right)\left(\cot\frac{\delta}{2}\right) - \left(\cot\frac{\delta}{2}\right)\left(\ln\sqrt{\cos^2\frac{\psi}{lU} + \sinh^2\frac{\varphi}{lU}}\right) + \arctan\left(\tanh\frac{\varphi}{lU}\tan\frac{\psi}{lU}\right)\right] \tag{B2}$$

Equations (B1) and (B2) are general equations in that they may be used to find the streamlines of a flow field with any angle of turning, since δ in the equations is the angle of bend. For this report $\delta = 60^\circ$. When mapping a streamline (ψ = constant) in the ξ,η-plane by equations (B1) and (B2), the velocity potential φ is considered as a variable parameter. A portion of the streamline pattern given by the equations is presented in figure 1.

Velocity. - Parametric equations for determining the velocity components of the flow field are obtained by differentiating equation (5) with respect to ζ and separating the real and imaginary parts. The real part is equal to the ξ-component of velocity and the imaginary part is the η-component of velocity. The results of this procedure are:

$$u_\xi = U\frac{\sinh 2\frac{\varphi}{lU} + \left(\cot^2\frac{\delta}{2}\right)\left(\cos 2\frac{\psi}{lU} + \cosh 2\frac{\varphi}{lU}\right) + \cot\frac{\delta}{2}\sin 2\frac{\psi}{lU}}{\left(\cot^2\frac{\delta}{2}\right)\left(\cosh 2\frac{\varphi}{lU} + \cos 2\frac{\psi}{lU}\right) + 2\cot\frac{\delta}{2}\sin 2\frac{\psi}{lU} - \cos 2\frac{\psi}{lU} + \cosh 2\frac{\varphi}{lU}} \tag{B3}$$

and

$$u_\eta = U\frac{\sin 2\frac{\psi}{lU} + \left(\cot\frac{\delta}{2}\right)\left(\cos 2\frac{\psi}{lU} + \cosh 2\frac{\varphi}{lU}\right) - \cot\frac{\delta}{2}\sinh 2\frac{\varphi}{lU}}{\left(\cot^2\frac{\delta}{2}\right)\left(\cosh 2\frac{\varphi}{lU} + \cos 2\frac{\psi}{lU}\right) + 2\cot\frac{\delta}{2}\sin 2\frac{\psi}{lU} - \cos 2\frac{\psi}{lU} + \cosh 2\frac{\varphi}{lU}} \tag{B4}$$

Equations (B3) and (B4) are also general in that they contain δ the angle of turning of the flow field. When the velocity components are determined along a streamline (ψ = constant) by these equations, the velocity potential φ is considered as a variable parameter.

Walls and ends of elbow. - It can be shown (ref. 14) that the flow field between the two streamlines $\psi = 15\pi lU/32$ and $l\pi U/12$ shown in figure 1 satisfies all the assumed criteria for a 60° elbow. The first condition is strictly fulfilled only at infinity, but the flow approaches uniform and rectilinear motion very rapidly before and after the bend. Therefore, the ends of the elbow may be selected at some reasonable distance before and after the bend without serious error. For this droplet study, the ends of the elbow are defined by the lines $\eta = -0.5774\xi - 0.866\pi l$ and $\xi = \frac{3}{4}\pi l$ (indicated by dashed lines in fig. 1). The error in assuming that the flow between streamlines $\psi = 15\pi lU/32$ and $\pi lU/12$ is uniform and rectilinear with free-stream velocity U at the entrance and exit is approximately 1 percent.

Since the flow field between the streamlines $\psi = \pi lU/12$ and $\psi = 15\pi lU/32$ satisfies the assumed criteria for an elbow, any pair of streamlines between these two may be selected as walls of a two-dimensional elbow. However, elbows defined by pairs of streamlines between $\psi = \pi lU/12$ and $\psi = 4\pi lU/12$ are probably the most practical elbows, because they more nearly approximate conventional elbows. Of all the possible elbows defined by pairs of streamlines between $\psi = \pi lU/12$ and $4\pi lU/12$, the most useful elbow is probably the elbow defined by these two streamlines, because for a given entrance width the average turning radius is smaller for this elbow than for any elbow defined by a pair of streamlines between these two, as is discussed in the next section. In this impingement study, the flow field of figure 1 is divided into three classes of elbows, basic, supplementary, and pocket, which are defined in the ANALYSIS section of the report.

Relation between l and elbow size. - The linear parameter l of the complex potential function (eq. (5)) is related to the size of the elbow through two quantities, the width of the entrance and a quantity that may be regarded as the turning radius of the elbow. The relation between the coordinates and the stream function ψ at $\xi = \infty$ is

$$\eta = \psi/U \tag{B5}$$

from which the spacing of streamlines (width of elbow) can be determined at infinity. For example, for the basic elbow defined by $\psi = \pi lU/12$ and $\psi = 4\pi lU/12$, the width of the elbow at $\xi = \infty$ is $\pi l/4$ or 0.7854, whereas the width of the elbow terminated at $\xi = \frac{3}{4}\pi l$ is 0.7900. The error in elbow entrance width caused by terminating the basic elbow at

$\xi = 3\pi l/4$ (fig. 1) and assuming that the elbow entrance width is $\pi l/4$ is less than 1 percent. Since this error is small, equation (B5) can be used to find the approximate width of any elbow defined by a pair of streamlines between $\psi = 15\pi lU/32$ and $\pi lU/4$.

The point A in figure 1 may be regarded as the center of turning for the elbows. The coordinates of this point are $\xi = \frac{3}{4}\pi l$ and $\eta = -\frac{3}{4}\pi l \cot 30^\circ$. A radius of turning of an elbow or any streamline may be defined as the distance from A, measured along the lines defining the ends of the elbow, to the elbow wall or streamline. The radius of turning for a particular wall or streamline is proportional to l and is determined by adding $\frac{3}{4}\pi l \cot 30^\circ$ to the distance between the wall or streamline and the ξ-axis. This distance can be approximated by equation (B5). For example, for the basic elbow, the average radius of turning may be defined as the distance from point A (fig. 1) to the midpoint of the entrance. The streamline $\psi = 5\pi lU/24$ defines the midpoint of the entrance, and the distance between this point and the ξ-axis is approximately $5\pi l/24$ (from eq. (B5)). The average turning radius for the basic elbow is therefore approximately equal to $\frac{3}{4}\pi l \cot 30^\circ + \frac{5\pi l}{24}$.

Inasmuch as the width of an elbow at the entrance and the radius of turning are both proportional to l, the basic elbow is probably the most practical elbow, because for a given entrance width (physical units such as feet) the turning radius is smaller for this elbow than for supplementary elbows.

Elbow cross section. - An elbow with any entrance cross-sectional configuration that satisfies all the criteria outlined in the body of this report may be designed by the use of equations (B1) and (B2). The only conditions to be satisfied are that those streamlines forming the walls of the elbow at the entrance must remain on the walls throughout the elbow and that the streamlines must be identical to or intermediate to $\psi = 15\pi lU/32$ and $\psi = \pi lU/4$. For an elbow with a rectangular entrance cross section, the cross sections at all points along the elbow are rectangular. However, the width of the elbow changes while the depth remains constant. For an elbow with a circular entrance cross section, the cross sections become egg-shaped in the center of the elbow. The depth, however, remains constant throughout the elbow.

Elbow and flow field in dimensionless form. - For droplet impingement studies for airfoils and other aircraft components, it is convenient to express the results in terms of dimensionless parameters, so that the results may apply to a wide range of flight and meteorlogical conditions as well as a wide range of sizes of airfoils and aircraft components. In order to obtain the impingement results in terms of dimensionless parameters by analog computer technique, the aircraft component and the flow

field must be expressed in terms of dimensionless parameters. This necessity is met for airfoils by expressing all distances as ratios to chord length and all velocities as ratios to free-stream velocity. The elbow and its velocity field can be expressed in dimensionless form by expressing distances as ratios to the arbitrary length l and velocities as ratios to the free-stream velocity U; thus for the elbow walls and intermediate streamlines, both sides of equations (B1) and (B2) are divided by l, and for the flow fields, both sides of equations (B3) and (B4) are divided by the free-stream velocity U.

Some typical streamlines are presented in terms of dimensionless coordinates in graphical form in figure 2 and in tabular form in table I. Figure 2 and table I, with the elbow entirely in the first quadrant, were obtained from figure 1 and equations (B1) and (B2) by the following transformation equations:

$$x = 0.866\ \xi - 0.5\ \eta + 2.00$$

and

$$y = 0.5\ \xi + 0.866\ \eta + 3.00$$

The translation of the origin was made in order to facilitate trajectory calculations by the differential analyzer.

The velocity field is presented in figure 3 and table I. Figure 3(a) gives the x-component velocity u_x as a function of x for constant values of y, and figure 3(b) gives the y-component of velocity u_y as a function y for constant values of x. The component velocities u_x and u_y are dimensionless and are equal to u_ξ/U and u_η/U, respectively.

REFERENCES

1. Brun, Rinaldo J., Serafini, John S., and Moshos, George J.: Impingement of Water Droplets on a NACA 65_1-212 Airfoil at an Angle of Attack of 4°. NACA RM E52B12, 1952.

2. Brun, Rinaldo J., Gallagher, Helen M., and Vogt, Dorothea E.: Impingement of Water Droplets on NACA 65_1-208 and 65_1-212 Airfoils at 4° Angle of Attack. NACA TN 2952, 1953.

3. Dorsch, Robert G., and Brun, Rinaldo J.: A Method for Determining Cloud-Droplet Impingement on Swept Wings. NACA TN 2931, 1953.

4. Brun, R. J., Lewis, W., Perkins, P. J., and Serafini, J. S.: Impingement of Cloud Droplets on a Cylinder and Procedure for Measuring Liquid-Water Content and Droplet Sizes in Supercooled Clouds by Rotating Multicylinder Method. NACA Rep. 1215, 1955. (Supersedes NACA TN's 2903, 2904, and NACA RM E53D23.)

5. Brun, Rinaldo J., Gallagher, Helen M., and Vogt, Dorothea E.: Impingement of Water Droplets on NACA 65A004 Airfoil and Effect of Change in Airfoil Thickness from 12 to 4 Percent at 4° Angle of Attack. NACA TN 3047, 1953.

6. Dorsch, Robert G., Brun, Rinaldo J., and Gregg, John L.: Impingement of Water Droplets on a Ellipsoid with Fineness Ratio 5 in Axisymmetric Flow. NACA TN 3099, 1954.

7. Brun, Rinaldo J., and Dorsch, Robert G.: Impingement of Water Droplets on an Ellipsoid with Fineness Ratio 10 in Axisymmetric Flow. NACA TN 3147, 1954.

8. Brun, Rinaldo J., Gallagher, Helen M., and Vogt, Dorothea E.: Impingement of Water Droplets on NACA 65A004 Airfoil at 8° Angle of Attack. NACA TN 3155, 1954.

9. Dorsch, Robert G., Saper, Paul G., and Kadow, Charles F.: Impingement of Water Droplet on a Sphere. NACA TN 3587, 1955.

10. Brun, Rinaldo J.: Cloud-Droplet Ingestion in Engine Inlets with Inlet Velocity Ratios of 1.0 and 0.7. NACA TN 3593, 1956.

11. Lewis, William, and Brun, Rinaldo J.: Impingement of Water Droplets on a Rectangular Half Body in a Two-Dimensional Incompressible Flow Field. NACA TN 3658, 1956.

12. Hacker, Paul T., Brun, Rinaldo J., and Boyd, Bemrose: Impingement of Droplets in 90° Elbows with Potential Flow. NACA TN 2999, 1953.

13. Langmuir, Irving, and Blodgett, Katherine B.: A Mathematical Investigation of Water Droplet Trajectories. Tech. Rep. No. 5418, Air Materiel Command, AAF, Feb. 19, 1946. (Contract No. W-33-038-ac-9151 with General Electric Co.)

14. Szczeniowski, Boleslaw: Design of Elbows in Potential Motion. Jour. Aero. Sci., vol. 11, no. 1, Jan. 1944, pp. 73-75.

15. Harper, John J.: Tests on Elbows of a Special Design. Jour. Aero. Sci., vol. 13, no. 11, Nov. 1946, pp. 587-592.

16. von Glahn, Uwe H., Gelder, Thomas F., and Smyers, William H., Jr.: A Dye-Tracer Technique for Experimentally Obtaining Impingement Characteristics of Arbitrary Bodies and a Method for Determining Droplet Size Distribution. NACA TN 3338, 1955.

TABLE I. - STREAMLINE COORDINATES, VELOCITY COMPONENTS, AND DISTANCE FROM ENTRANCE AS FUNCTIONS OF VELOCITY POTENTIAL

Velocity potential, ϕ/iU	Stream function, ψ														
	Streamline coordinate		Velocity component		Distance from entrance, S	Streamline coordinate		Velocity component		Distance from entrance, S	Streamline coordinate		Velocity component		Distance from entrance, S
	x	y	u_x	u_y		x	y	u_x	u_y		x	y	u_x	u_y	
	$15\pi iU/32$					$14\pi iU/32$					$13\pi iU/32$				
Entrance	-0.5239	0.6438	-0.0068	0.9939	0	0.6228	0.6438	-0.0055	0.9928	0	0.7217	0.6438	-0.0039	0.9919	0
-2.2	.5227	.8041	-.0092	.0018	.157	.6218	.8049	-.0074	.9902	.158	.7210	.8055	-.0053	.9889	.158
-2.0	.5204	1.0061	-.0136	.9876	.358	.6200	1.0074	-.0109	.9852	.358	.7197	1.0083	-.0078	.9834	.359
-1.8	.5170	1.2092	-.0202	.9813	.562	.6172	1.2110	-.0161	.9778	.562	.7177	1.2125	-.0114	.9752	.565
-1.6	.5118	1.4138	-.0299	.9716	.768	.6131	1.4166	-.0236	.9665	.768	.7148	1.4187	-.0165	.9629	.772
-1.4	.5039	1.6208	-.0441	.9565	.970	.6068	1.6250	-.0342	.9493	.973	.7104	1.6282	-.0234	.9443	.976
-1.2	.4919	1.8317	-.0643	.9327	1.182	.5974	1.8381	-.0489	.9227	1.186	.7040	1.8428	-.0324	.9162	1.192
-1.0	.4735	2.0487	-.0922	.8944	1.402	.5832	2.0586	-.0677	.8815	1.410	.6947	2.0655	-.0425	.8740	1.416
-.8	.4446	2.2761	-.1279	.8315	1.633	.5618	2.2915	-.0887	.8173	1.644	.6815	2.3017	-.0506	.8112	1.654
-.6	.3981	2.5227	-.1649	.7281	1.883	.5294	2.5469	-.1035	.7191	1.902	.6644	2.5611	-.0484	.7208	1.913
-.4	.3199	2.8095	-.1785	.5649	2.182	.4828	2.8475	-.0910	.5782	2.210	.6479	2.8628	-.0190	.6002	2.218
-.2	.1841	3.2088	-.1128	.3454	2.604	.4368	3.2514	-.0148	.4064	2.614	.6616	3.2397	.0603	.4627	2.595
-.1	.1036	3.5380	-.0306	.2356	2.943	.4529	3.5251	.0564	.3240	2.886	.7090	3.4621	.1229	.3983	2.819
.1	.5859	4.3734	.2190	.0911	3.981	.7717	4.0773	.2524	.2108	3.535	.9544	3.8870	.2835	.3056	3.309
.2	.9113	4.4682	.3555	.0750	4.320	1.0007	4.2282	.3594	.1903	3.807	1.1233	4.0393	.3705	.2835	3.533
.4	1.3249	4.5503	.5785	.1279	4.742	1.3735	4.3902	.5463	.2103	4.211	1.4428	4.2396	.5293	.2837	3.910
.6	1.6124	4.6260	.7130	.2213	5.041	1.6571	4.5001	.6745	.2699	4.519	1.7123	4.3762	.6484	.3185	4.215
.8	1.8492	4.7090	.7840	.3050	5.291	1.8945	4.5998	.7521	.3318	4.777	1.9455	4.4910	.7278	.3618	4.474
1.0	2.0607	4.7977	.8206	.3673	5.522	2.1070	4.6977	.7972	.3821	5.011	2.1566	4.5977	.7781	.4002	4.712
1.2	2.2578	4.8902	.8399	.4107	5.742	2.3050	4.7957	.8235	.4190	5.235	2.3542	4.7010	.8096	.4301	4.936
1.4	2.4464	4.9853	.8504	.4401	5.954	2.4942	4.8940	.8342	.4450	5.448	2.5432	4.8027	.8295	.4518	5.152
1.6	2.6296	5.0819	.8564	.4599	6.156	2.6778	4.9929	.8488	.4628	5.653	2.7268	4.9037	.8421	.4672	5.356
1.8	2.8094	5.1798	.8599	.4731	6.362	2.8579	5.0921	.8549	.4750	5.859	2.9069	5.0043	.8503	.4777	5.563
2.0	2.9870	5.2783	.8621	.4820	6.566	3.0357	5.1915	.8587	.4832	6.063	3.0847	5.1046	.8556	.4850	5.769
2.2	3.1631	5.3774	.8635	.4879	6.767	3.2120	5.2911	.8612	.4887	6.263	3.2610	5.2049	.8591	.4899	5.970
Exit	3.3025	5.4565	.8642	.4911	6.924	3.3520	5.3709	.8625	.4917	6.421	3.4014	5.2851	.8609	.4925	6.128
	$12\pi iU/32$					$11\pi iU/32$					$4\pi iU/12$				
Entrance	0.8207	0.6438	-0.0023	0.9913	0	0.9198	0.6438	-0.0005	0.9910	0	0.9528	0.6438	0.0001	0.0010	0
-2.2	.8204	.8060	-.0030	.9881	.158	.9197	.8062	-.0007	.9878	.158	.9529	.8062	.0001	.9878	.158
-2.0	.8196	1.0089	-.0044	.9823	.359	.9196	1.0092	-.0009	.9819	.360	.9529	1.0092	.0003	.9819	.360
-1.8	.8185	1.2133	-.0063	.9736	.564	.9193	1.2137	-.0011	.9730	.566	.9530	1.2138	.0006	.9731	.567
-1.6	.8168	1.4201	-.0089	.9607	.773	.9191	1.4206	-.0012	.9600	.773	.9532	1.4206	.0014	.9601	.773
-1.4	.8145	1.6302	-.0121	.9415	.979	.9189	1.6309	-.0007	.9409	.980	.9537	1.6308	.0030	.9409	.980
-1.2	.8113	1.8456	-.0155	.9130	1.194	.9188	1.8464	.0011	.9130	1.194	.9547	1.8463	.0065	.9137	1.194
-1.0	.8071	2.0694	-.0176	.8715	1.418	.9196	2.0701	.0062	.8733	1.418	.9572	2.0698	.0137	.8748	1.419
-.8	.8023	2.3066	-.0148	.8119	1.653	.9229	2.3063	.0181	.8181	1.653	.9628	2.3052	.0284	.8211	1.651
-.6	.7996	2.5655	.0005	.7303	1.913	.9325	2.5615	.0434	.7451	1.913	.9759	2.5622	.0564	.7511	1.908
-.4	.8077	2.8598	.0408	.6270	2.213	.9592	2.8442	.0909	.6565	2.198	1.0076	2.8370	.1059	.6667	2.188
-.2	.8557	3.2040	.1201	.5145	2.560	1.0257	3.1583	.1691	.5625	2.515	1.0782	3.1420	1.1836	.5778	2.500
-.1	.9126	3.3915	.1760	.4623	2.753	1.0847	3.3226	.2201	.5188	2.687	1.1371	3.2996	.2332	.5364	2.665
.1	1.1172	3.7460	.3124	.3836	3.162	1.2635	3.6317	.3393	.4500	3.042	1.3092	3.5976	.3479	.4702	3.010
.2	1.2512	3.8891	.3855	.3612	3.355	1.3758	3.7647	.4026	.4276	3.214	1.4161	3.7273	.4086	.4479	3.175
.4	1.5253	4.1027	.5226	.3489	3.702	1.6145	3.9793	.5231	.4070	3.531	1.6450	3.9410	.5245	.4251	3.487
.6	1.7761	4.2569	.6322	.3656	4.002	1.8460	4.1438	.6236	.4101	3.816	1.8706	4.1078	.6222	.4244	3.767
.8	2.0017	4.3839	.7105	.3931	4.262	2.0622	4.2797	.6994	.4247	4.076	2.0832	4.2457	.6969	.4352	4.024
1.0	2.2095	4.4984	.7635	.4205	4.497	2.2652	4.4006	.7532	.4420	4.311	2.2842	4.3683	.7507	.4493	4.256
1.2	2.4054	4.6066	.7985	.4431	4.721	2.4585	4.5131	.7902	.4575	4.535	2.4765	4.4821	.7880	.4625	4.481
1.4	2.5936	4.7116	.8214	.4602	4.936	2.6451	4.6209	.8152	.4698	4.749	2.6626	4.5908	.8135	.4732	4.695
1.6	2.7767	4.8146	.8364	.4726	5.142	2.8274	4.7258	.8320	.4790	4.956	2.8444	4.6963	.8308	.4812	4.902
1.8	2.9366	4.9166	.8464	.4813	5.351	3.0066	4.8291	.8432	.4856	5.163	3.0234	4.7999	.8424	.4871	5.108
2.0	3.1341	5.0178	.8529	.4873	5.556	3.1839	4.9311	.8508	.4902	5.369	3.2006	4.9022	.8502	.4912	5.315
2.2	3.3103	5.1186	.8573	.4914	5.757	3.3598	5.0325	.8558	.4933	5.571	3.3764	5.0038	.8553	.4940	5.517
Exit	3.4509	5.1988	.8596	.4936	5.915	3.5004	5.1136	.8585	.4951	5.729	3.5170	5.0850	.8582	.4956	5.675

TABLE I. - Continued. STREAMLINE COORDINATES, VELOCITY COMPONENTS, AND DISTANCE FROM ENTRANCE AS FUNCTIONS OF VELOCITY POTENTIAL

Velocity potential, ϕ/iU	Stream function, ψ													
	Streamline coordinate		Velocity component		Distance from entrance, S	Streamline coordinate		Velocity component		Distance from entrance, S	Streamline coordinate		Velocity component		Distance from entrance, S
	x	y	u_x	u_y		x	y	u_x	u_y		x	y	u_x	u_y	
	$10\pi l U/32$					$9\pi l U/32$					$8\pi l U/32$				
Entrance	1.0187	0.6438	0.0012	0.9911	0	1.1179	0.6438	0.0030	0.9915	0	1.2169	0.6438	0.0045	0.9922	0
-2.2	1.0191	.8061	.0017	.9879	.158	1.1184	.8058	.0040	.9885	.157	1.2177	.8053	.0061	.9895	.157
-2.0	1.0196	1.0091	.0026	.9821	.360	1.1194	1.0086	.0060	.9830	.360	1.2192	1.0079	.0092	.9845	.361
-1.8	1.0202	1.2136	.0041	.9734	.567	1.1210	1.2129	.0091	.9748	.566	1.2216	1.2117	.0137	.9771	.564
-1.6	1.0213	1.4203	.0064	.9608	.772	1.1234	1.4192	.0137	.9629	.772	1.2252	1.4174	.0203	.9663	.771
-1.4	1.0232	1.6303	.0103	.9423	.978	1.1271	1.6286	.0208	.9457	.976	1.2306	1.6258	.0303	.9508	.972
-1.2	1.0262	1.8459	.0170	.9159	1.193	1.1330	1.8425	.0317	.9214	1.192	1.2390	1.8381	.0450	.9290	1.186
-1.0	1.0317	2.0679	.0283	.8788	1.418	1.1427	2.0631	.0486	.8876	1.142	1.2522	2.0560	.0667	.8991	1.405
-.8	1.0420	2.3014	.0479	.8286	1.647	1.1589	2.2929	.0745	.8426	1.639	1.2830	2.2813	.0986	.8596	1.626
-.6	1.0619	2.5508	.0809	.7640	1.900	1.1866	2.5351	.1136	.7859	1.882	1.3066	2.5158	.1421	.8101	1.862
-.4	1.1013	2.8204	.1335	.6876	2.172	1.2346	2.7916	.1700	.7196	2.143	1.3600	2.7599	.2018	.7525	2.114
-.2	1.1776	3.1090	.2104	.6075	2.472	1.3156	3.0589	.2461	.6503	2.423	1.4426	3.0093	.2775	.6916	2.379
-.1	1.2359	3.2557	.2577	.5700	2.613	1.3722	3.1927	.2908	.6173	2.568	1.4972	3.1330	.3205	.6619	2.511
.1	1.3966	3.5339	.3648	.5082	2.960	1.5193	3.4474	.3892	.5605	2.858	1.6334	3.3690	.4130	.6085	2.783
.2	1.4944	3.6577	.4209	.4859	3.101	1.6068	3.5633	.4401	.5382	3.003	1.7133	3.4781	.4602	.5861	2.915
.4	1.7062	3.8682	.5287	.4594	3.401	1.7978	3.7671	.5382	.5071	3.283	1.8879	3.6744	.5508	.5510	3.180
.6	1.9200	4.0371	.6213	.4520	3.673	1.9959	3.9369	.6238	.4913	3.544	2.0726	3.8426	.6305	.5281	3.432
.8	2.1260	4.1790	.6936	.4558	3.926	2.1919	4.0820	.6925	.4859	3.787	2.2590	3.9889	.6954	.5147	3.668
1.0	2.3231	4.3046	.7469	.4640	4.155	2.3828	4.2109	.7444	.4859	4.014	2.4436	4.1197	.7453	.5073	3.889
1.2	2.5131	4.4206	.7847	.4726	4.380	2.5690	4.3296	.7821	.4881	4.234	2.6258	4.2400	.7821	.5035	4.110
1.4	2.6978	4.5308	.8109	.4801	4.695	2.7512	4.4417	.8086	.4909	4.450	2.8054	4.3534	.8083	.5017	4.324
1.6	2.8788	4.6374	.8288	.4859	4.801	2.9307	4.5496	.8271	.4933	4.654	2.9832	4.4624	.8267	.5008	4.525
1.8	3.0572	4.7417	.8410	.4902	5.006	3.1082	4.6548	.8397	.4952	4.860	3.1595	4.5683	.8393	.5004	4.732
2.0	3.2340	4.8446	.8492	.4933	5.213	3.2843	4.7583	.8483	.4967	5.066	3.3348	4.6722	.8480	.5002	4.935
2.2	3.4096	4.9465	.8547	.4954	5.415	3.4595	4.8606	.8541	.4977	5.269	3.5095	4.7748	.8539	.5001	5.139
Exit	3.5500	5.0278	.8577	.4966	5.573	3.5995	4.9420	.8572	.4983	5.426	3.6490	4.8563	.8571	.5000	5.296
	$7\pi l U/32$					$6\pi l U/32$					$5\pi l U/32$				
Entrance	1.3158	0.6438	0.0059	0.9933	0	1.4145	0.6438	0.0071	0.9945	0	1.5132	0.6438	0.0079	0.9960	0
-2.2	1.3169	.8046	.0080	.9909	.157	1.4158	.8037	.0096	.9926	.156	1.5146	.8027	.0109	.9946	.156
-2.0	1.3189	1.0068	.0119	.9865	.358	1.4183	1.0055	.0143	.9891	.358	1.5174	1.0040	.0161	.9920	.358
-1.8	1.3219	1.2101	.0177	.9801	.562	1.4219	1.2082	.0212	.9839	.561	1.5214	1.2058	.0238	.9882	.559
-1.6	1.3265	1.4150	.0262	.9708	.766	1.4272	1.4120	.0312	.9763	.766	1.5274	1.4086	.0351	.9826	.761
-1.4	1.3334	1.6221	.0387	.9575	.970	1.4353	1.6176	.0458	.9654	.965	1.5363	1.6126	.0513	.9745	.960
-1.2	1.3438	1.8324	.0565	.9387	1.177	1.4474	1.8257	.0666	.9806	1.172	1.5494	1.8181	.0744	.9628	1.165
-1.0	1.3598	2.0471	.0825	.9130	1.394	1.4655	2.0369	.0958	.9289	1.385	1.5696	2.2057	.1065	.9464	1.374
-.8	1.3843	2.2674	.1184	.8790	1.614	1.4925	2.2520	.1357	.9006	1.600	1.5975	2.2355	.1499	.9240	1.586
-.6	1.4218	2.4942	.1668	.8364	1.844	1.5324	2.4711	.1881	.8645	1.823	1.6387	2.4472	.2061	.8945	1.802
-.4	1.4783	2.7268	.2295	.7863	2.082	1.5904	2.6930	.2539	.8211	2.051	1.6968	2.6594	.2754	.8572	2.020
-.2	1.5606	2.9610	.3057	.7320	2.334	1.6714	2.9140	.3315	.7723	2.290	1.7757	2.8688	.3553	.8130	2.244
-.1	1.6131	3.0762	.3479	.7048	2.456	1.7216	3.0224	.3735	.7469	2.404	1.8238	2.9710	.3979	.7890	2.356
.1	1.7405	3.2970	.4365	.6537	2.708	1.8414	3.2300	.4601	.6969	2.645	1.9376	3.1671	.4843	.7391	2.526
.2	1.8141	3.4000	.4811	.6307	2.830	1.9101	3.3276	.5031	.6732	2.759	2.0014	3.2598	.5264	.7142	2.688
.4	1.9758	3.5884	.5662	.5919	3.082	2.0611	3.5083	.5841	.6304	2.998	2.1434	3.4329	.6047	.6671	2.912
.6	2.1489	3.7537	.6409	.5627	3.320	2.2242	3.6694	.6546	.5952	3.226	2.2981	3.5893	.6716	.6257	3.130
.8	2.3266	3.8996	.7021	.5420	3.550	2.3941	3.8136	.7121	.5678	3.449	2.4608	3.7308	.7253	.5918	3.346
1.0	2.5051	4.0309	.7494	.5279	3.770	2.5669	3.9445	.7565	.5474	3.664	2.6283	3.8605	.7664	.5655	3.558
1.2	2.6831	4.1520	.7846	.5185	3.987	2.7407	4.0658	.7895	.5327	3.877	2.7983	3.9812	.7966	.5458	3.767
1.4	2.8600	4.2663	.8099	.5123	4.194	2.9148	4.1803	.8132	.5223	4.094	2.9697	4.0954	.8182	.5317	3.972
1.6	3.0359	4.3758	.8276	.5081	4.398	3.0889	4.2901	.8299	.5152	4.293	3.1419	4.2056	.8334	.5217	4.171
1.8	3.2110	4.4822	.8399	.5054	4.602	3.2627	4.3966	.8415	.5103	4.498	3.3145	4.3116	.8439	.5147	4.373
2.0	3.3856	4.5865	.8484	.5036	4.806	3.4364	4.5011	.8494	.5069	4.701	3.4873	4.4160	.8511	.5100	4.574
2.2	3.5597	4.6894	.8541	.5024	5.007	3.6100	4.6041	.8548	.5047	4.903	3.6602	4.5190	.8559	.5067	4.776
Exit	3.6985	4.7707	.8572	.5018	5.164	3.7478	4.6647	.8577	.5034	5.059	3.8070	4.5996	.8585	.5048	4.932

TABLE I. - Concluded. STREAMLINE COORDINATES, VELOCITY COMPONENTS, AND DISTANCE FROM ENTRANCE AS FUNCTIONS OF VELOCITY POTENTIAL

Velocity potential, ϕ/lU	Stream function, ψ														
	Streamline coordinate		Velocity component		Distance from entrance, S	Streamline coordinate		Velocity component		Distance from entrance, S	Streamline coordinate		Velocity component		Distance from entrance, S
	x	y	u_x	u_y		x	y	u_x	u_y		x	y	u_x	u_y	
	$4\pi lU/32$					$3\pi lU/32$					$\pi lU/12$				
Entrance	1.6117	0.6438	0.0087	0.9977	0	1.7100	0.6438	0.0090	0.9993	0	1.7428	0.6438	0.0088	1.0000	0
-2.2	1.6132	.8016	.0117	.9968	.156	1.7116	.8004	.0121	.9991	.155	1.7444	.8000	.0121	.9999	.155
-2.0	1.6161	1.0023	.0174	.9953	.358	1.7146	1.0006	.0180	.9987	.357	1.7473	.9999	.0180	.9998	.356
-1.8	1.6204	1.2034	.0257	.9929	.557	1.7190	1.2008	.0266	.9979	.555	1.7517	1.1999	.0267	.9996	.555
-1.6	1.6268	1.4049	.0378	.9895	.758	1.7255	1.4011	.0392	.9967	.755	1.7582	1.3998	.0394	.9992	.755
-1.4	1.6362	1.6071	.0552	.9843	.957	1.7351	1.6014	.0574	.9949	.951	1.7678	1.5996	.0577	.9983	.952
-1.2	1.6501	1.8101	.0801	.9767	1.158	1.7492	1.8018	.0834	.9914	1.150	1.7819	1.7991	.0840	.9965	1.148
-1.0	1.6703	2.0139	.1145	.9656	1.363	1.7695	2.0020	.1197	.9857	1.352	1.8021	1.9981	.1207	.9927	1.348
-.8	1.6995	2.2185	.1610	.9492	1.570	1.7986	2.2015	.1688	.9761	1.552	1.8310	2.1959	.1706	.9853	1.548
-.6	1.7410	2.4232	.2209	.9263	1.779	1.8394	2.3995	.2325	.9601	1.755	1.8714	2.3918	.2355	.9719	1.749
-.4	1.7982	2.6264	.2941	.8950	1.989	1.8949	2.5944	.3104	.9351	1.958	1.9262	2.5841	.3152	.9490	1.950
-.2	1.8744	2.8254	.3777	.8549	2.205	1.9680	2.7839	.3990	.8988	2.164	1.9982	2.7706	.4059	.9139	2.149
-.1	1.9202	2.9222	.4217	.8318	2.310	2.0117	2.8758	.4452	.8762	2.264	2.0411	2.8608	.4531	.8915	2.248
.1	2.0275	3.1080	.5095	.7811	2.518	2.1134	3.0520	.5362	.8237	2.470	2.1411	3.0340	.5455	.8381	2.452
.2	2.0884	3.1961	.5515	.7546	2.623	2.1712	3.1357	.5788	.7949	2.570	2.1978	3.1096	.5886	.8085	2.551
.4	2.2226	3.3616	.6281	.7022	2.839	2.2987	3.2938	.6546	.7363	2.776	2.3233	3.2719	.6643	.7475	2.760
.6	2.3700	3.5128	.6917	.6545	3.049	2.4397	3.4394	.7153	.6814	2.979	2.4624	3.4155	.7239	.6899	2.961
.8	2.5265	3.6510	.7416	.6140	3.258	2.5908	3.5737	.7609	.6342	3.182	2.6118	3.5484	.7680	.6404	3.162
1.0	2.6895	3.7786	.7789	.5819	3.465	2.7490	3.6987	.7938	.5965	3.382	2.7688	3.6723	.7993	.6009	3.362
1.2	2.8556	3.8980	.8058	.5577	3.670	2.9122	3.8113	.8169	.5679	3.584	2.9310	3.7894	.8210	.5709	3.562
1.4	3.0244	4.0115	.8248	.5400	3.871	3.0787	3.9287	.8328	.5471	3.783	3.0967	3.9013	.8357	.5492	3.758
1.6	3.1948	4.1208	.8380	.5274	4.070	3.2474	4.0372	.8436	.5323	3.979	3.2649	4.0095	.8457	.5337	3.955
1.8	3.3662	4.2271	.8471	.5187	2.471	3.4176	4.1430	.8509	.5220	4.179	3.4348	4.1151	.8524	.5229	4.155
2.0	3.5381	4.3313	.8532	.5127	4.470	3.5888	4.2470	.8559	.5149	4.377	3.6057	4.2189	.8569	.5155	4.354
2.2	3.7105	4.4342	.8574	.5086	4.672	3.7607	4.3496	.8592	.5101	4.579	3.7774	4.3214	.8599	.5105	4.555
Exit	3.8464	4.5144	.8596	.5065	4.828	3.8955	4.4292	.8610	.5075	4.734	3.9119	4.4008	.8615	.5078	4.710

TABLE II. - EXAMPLES OF INERTIA PARAMETER AND FREE-STREAM REYNOLDS NUMBER IN TERMS OF WIDTH OF BASIC ELBOW, FREE-STREAM VELOCITY, AIR DENSITY, AND DROPLET DIAMETER

Elbow entrance width, L, ft	Arbitrary length parameter, l, ft	Free-stream or entrance velocity, U, mph	Pressure altitude, ft	Air density, ρ_a, $\frac{\text{slugs}}{\text{cu ft}}$	Temperature, $^{\circ}F$	Air viscosity, μ, $\frac{\text{slugs}}{(\text{ft})(\text{sec})}$	Droplet diameter, d, microns	Inertia parameter, K	Free-stream Reynolds number, Re_0	Maximum extent of impingement for basic elbow, S_m	Collection efficiency for basic elbow, E'
0.5	0.6366	200	10×10^3	1.756×10^{-3}	12	34.54×10^{-8}	10	0.1549	48.9	5.68	0.13
.5	.6366	200	10	1.756	12	34.54	25	.9676	122.3	5.68	.52
.5	.6366	200	30	.889	-39	31.43	10	.1704	27.2	5.68	.14
.5	.6366	200	30	.889	-39	31.43	25	1.0650	68.1	5.68	.65
.5	.6366	500	10	1.756	12	34.54	10	.3872	122.3	5.68	.24
.5	.6366	500	10	1.756	12	34.54	25	2.4180	305.8	5.68	.82
.5	.6366	500	30	.889	-39	31.43	10	.4260	68.1	5.68	.28
.5	.6366	500	30	.889	-39	31.43	25	2.6625	170.2	4.72	1.00
1.0	1.2732	200	10	1.756	12	34.54	10	.0774	48.9	5.08	.06
1.0	1.2732	200	10	1.756	12	34.54	25	.4838	122.3	5.68	.29
1.0	1.2732	200	30	.889	-39	31.43	10	.0852	27.2	5.68	.07
1.0	1.2732	200	30	.889	-39	31.43	25	.5325	68.1	5.68	.32
1.0	1.2732	500	10	1.756	12	34.54	10	.1936	122.3	5.68	.13
1.0	1.2732	500	10	1.756	12	34.54	25	1.2090	305.8	5.68	.47
1.0	1.2732	500	30	.889	-39	31.43	10	.2130	68.1	5.68	.14
1.0	1.2732	500	30	.889	-39	31.43	25	1.3312	170.2	5.68	.61

TABLE III. - COMPARISON OF COLLECTION EFFICIENCIES OF THREE 60° ELBOWS AND BASIC 90° ELBOW OF REFERENCE 12

Inertia parameter, K	Free-stream Reynolds number, Re_0															
	0	0	0	0	32	32	32	32	128	128	128	128	512	512	512	512
	Elbow angle and type															
	60°			90°	60°			90°	60°			90°	60°			90°
	Basic	Pocket type A	Pocket type B	Basic	Basic	Pocket type A	Pocket type B	Basic	Basic	Pocket type A	Pocket type B	Basic	Basic	Pocket type A	Pocket type B	Basic
	Collection efficiency															
1/3	0.31	0	0	0.27	0.24	0	0	0.21	0.21	0	0	0.17	0.13	0	0	0.13
4/7	.54	0	0	.53	.40			.37	.34	0	0	.28	.21	0	0	.19
1	1.00	.53	.34	1.00	.73	.12	.08	.77	.52	.07	.04	.48	.35	0	0	.32
2	1.00	1.00	1.00	1.00	1.00	1.00	.75	1.00	.99	.34	.22	1.00	.62	.14	.09	.59
4	1.00	1.00	1.00	1.00	1.00	1.00	1100	1.00	1.00	1.00	.95	1.00	1.00	.55	.36	1.00
8	1.00	1.00	1.00	1.00	1.00	1.00	1.00	1.00	1.00	1.00	1.00	1.00	1.00	1.00	1.00	1.00

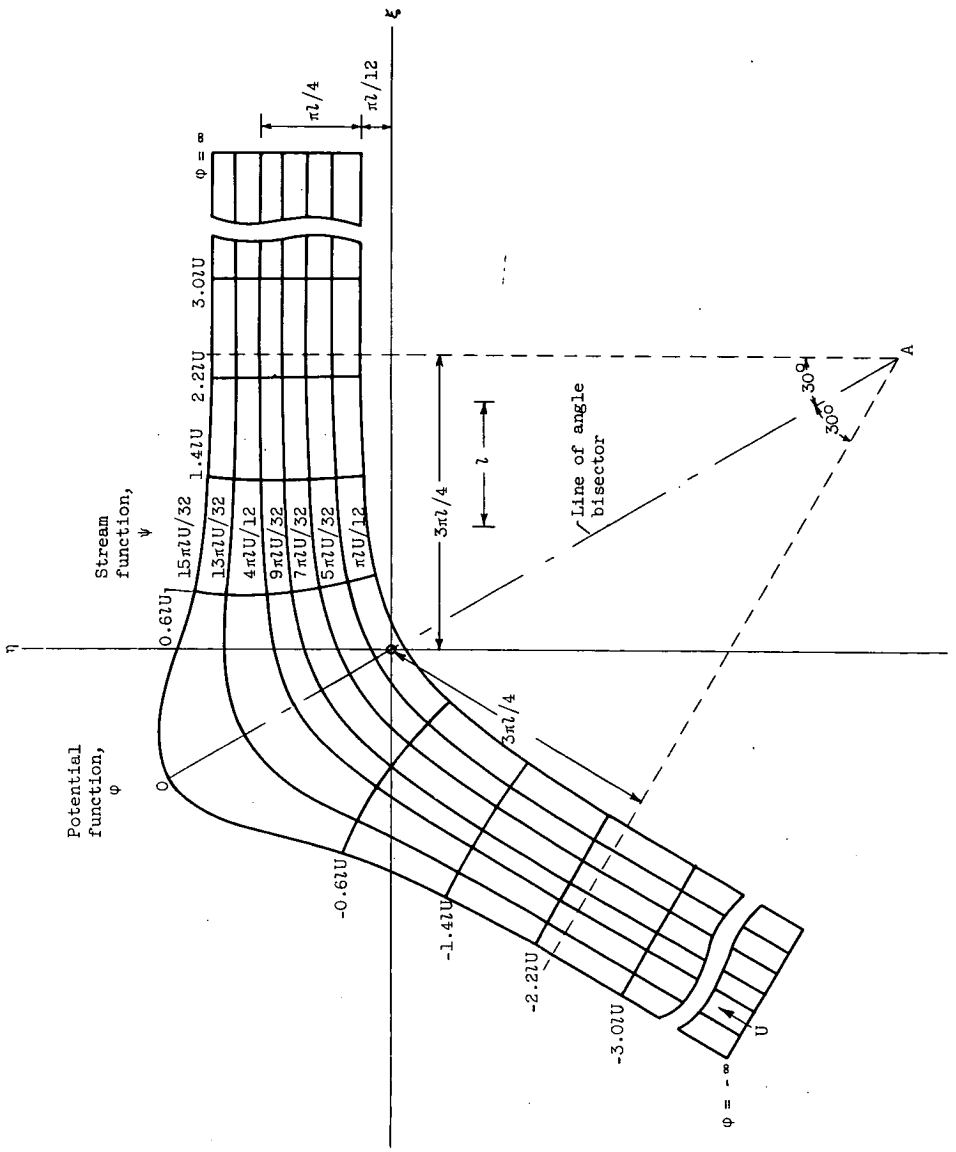

Figure 1. - Flow-field streamlines and constant-potential lines obtained from potential theory by equation (5).

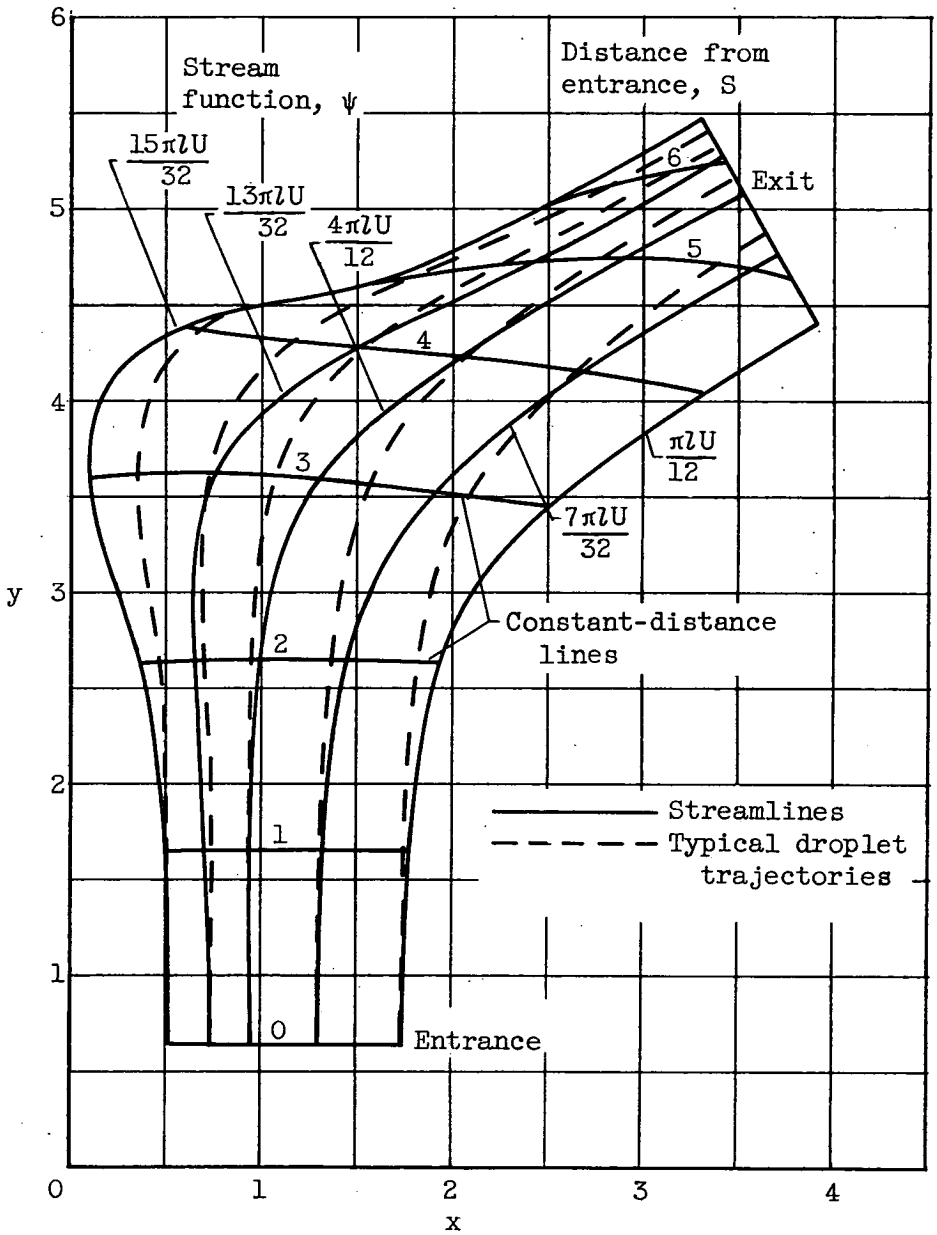

Figure 2. - Elbow with some typical streamlines and droplet trajectories.

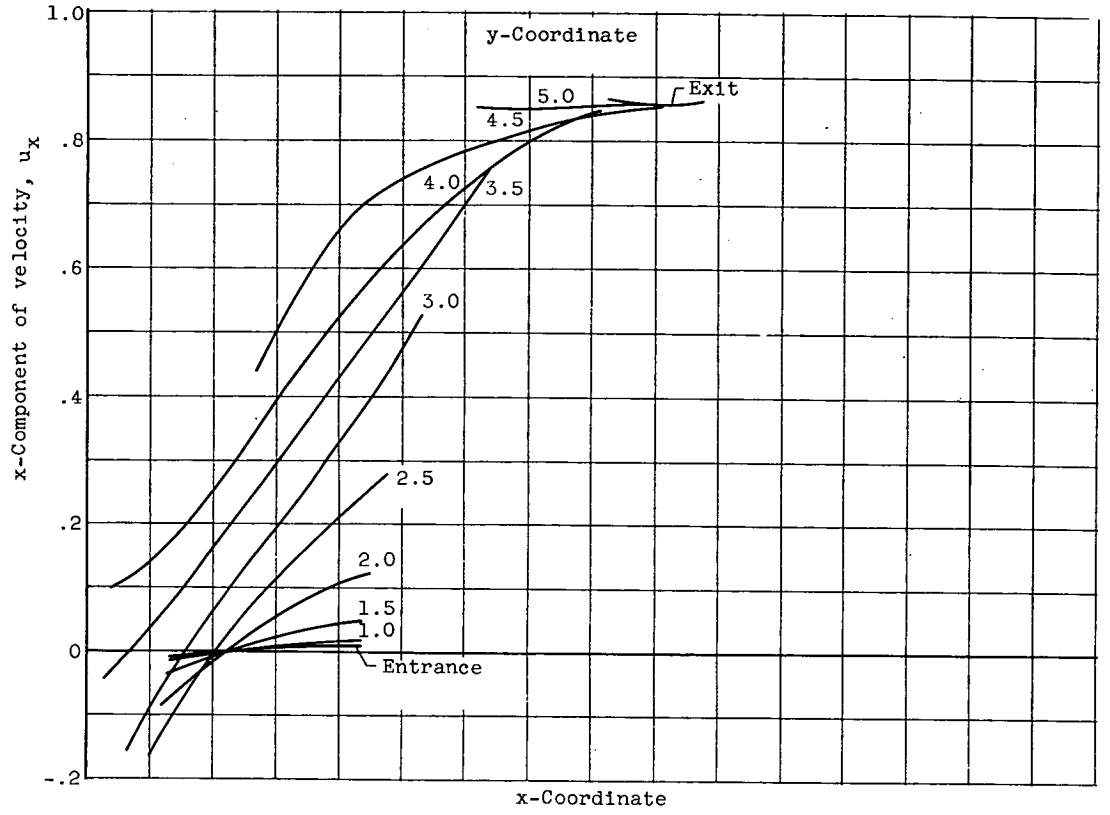

(a) x-Component of velocity.

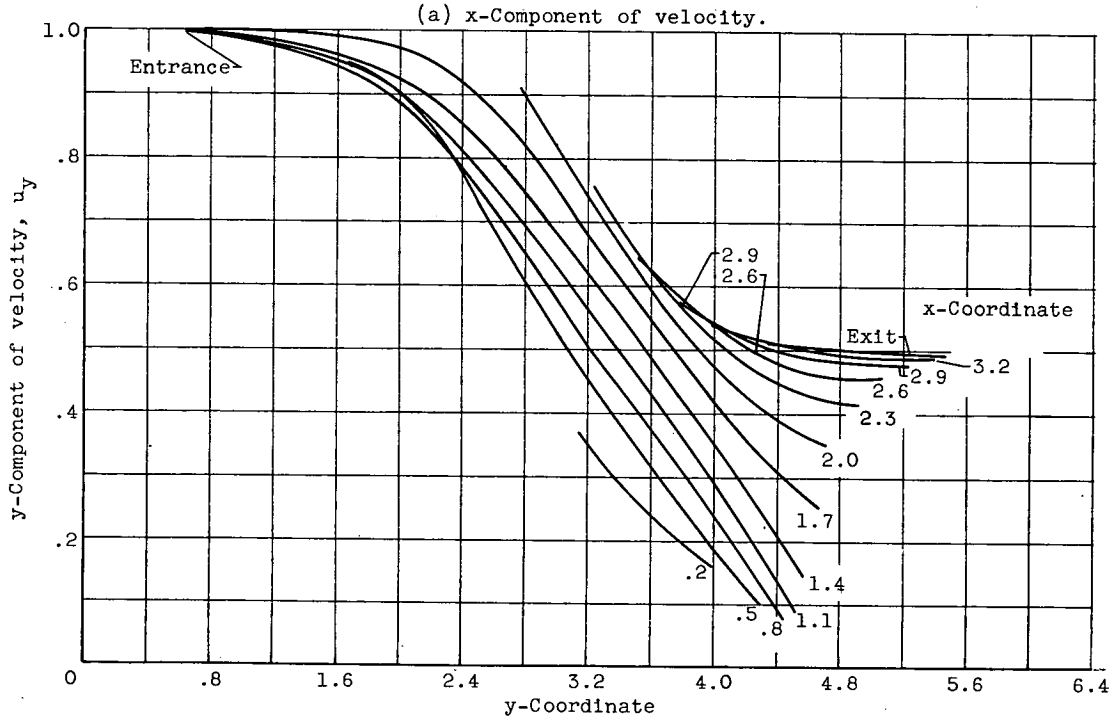

(b) y-Component of velocity.

Figure 3. - Elbow flow field.

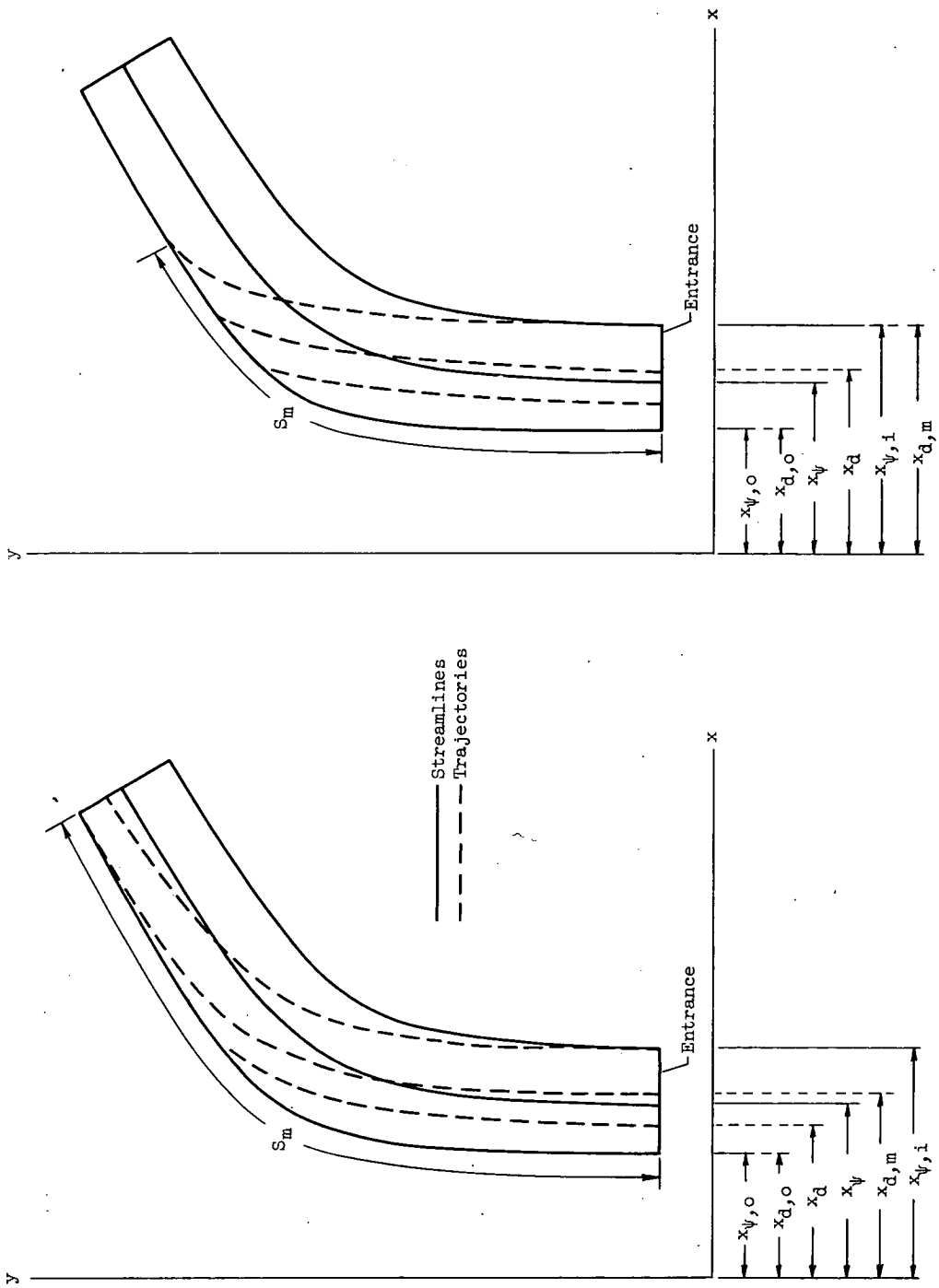

(a) Point of maximum extent of impingement at elbow exit.

(b) Point of maximum extent of impingement before elbow exit.

Figure 4. - Notation for streamlines and trajectories for basic and supplementary elbows.

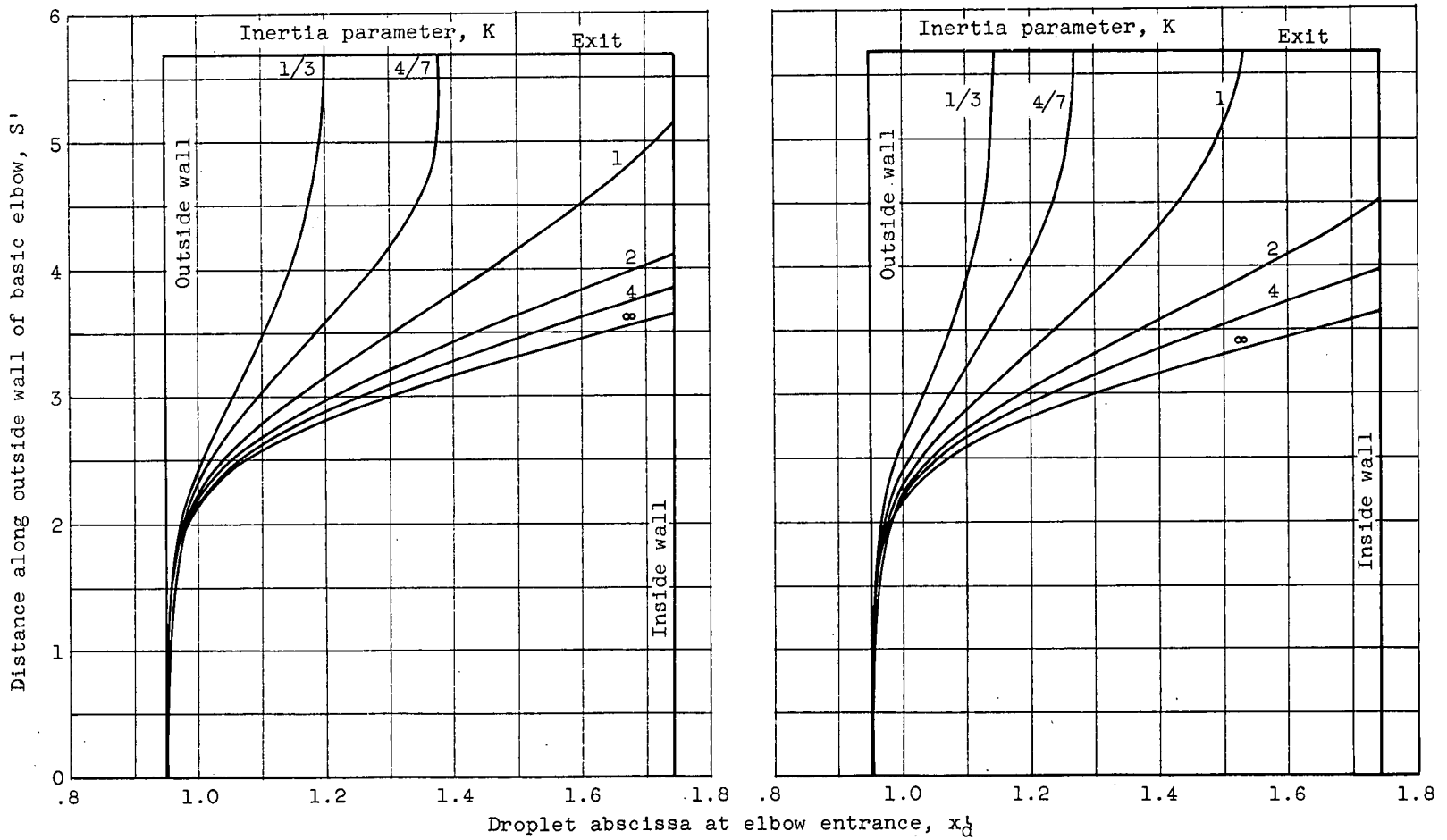

(a) Free-stream Reynolds number, 0.

(b) Free-stream Reynolds number, 32.

Figure 5. - Point of droplet impingement on outside wall of basic elbow as function of droplet abscissa at elbow entrance.

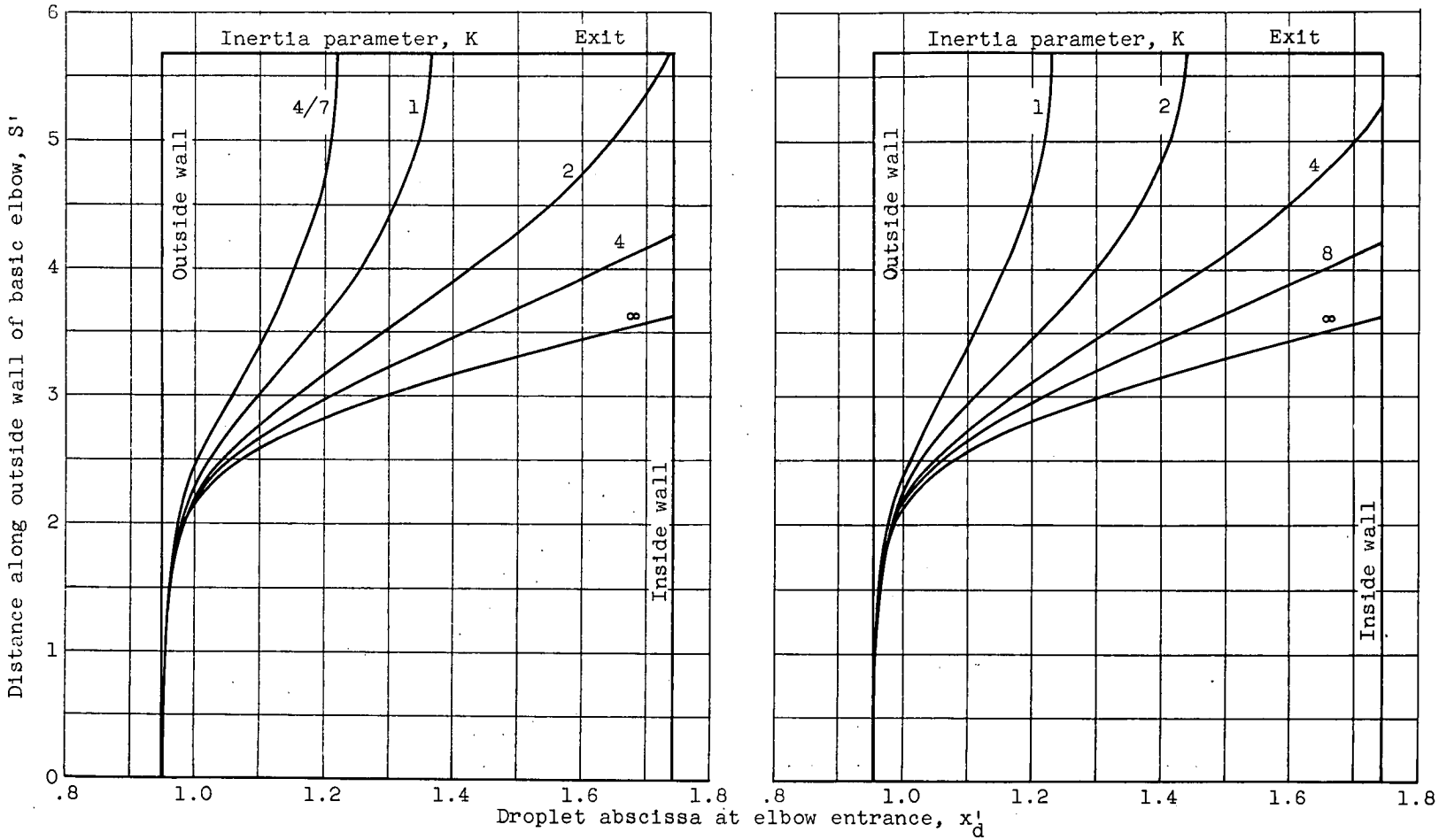

(c) Free-stream Reynolds number, 128.

(d) Free-stream Reynolds number, 512.

Figure 5. - Concluded. Point of droplet impingement on outside wall of basic elbow as function of droplet abscissa at elbow entrance.

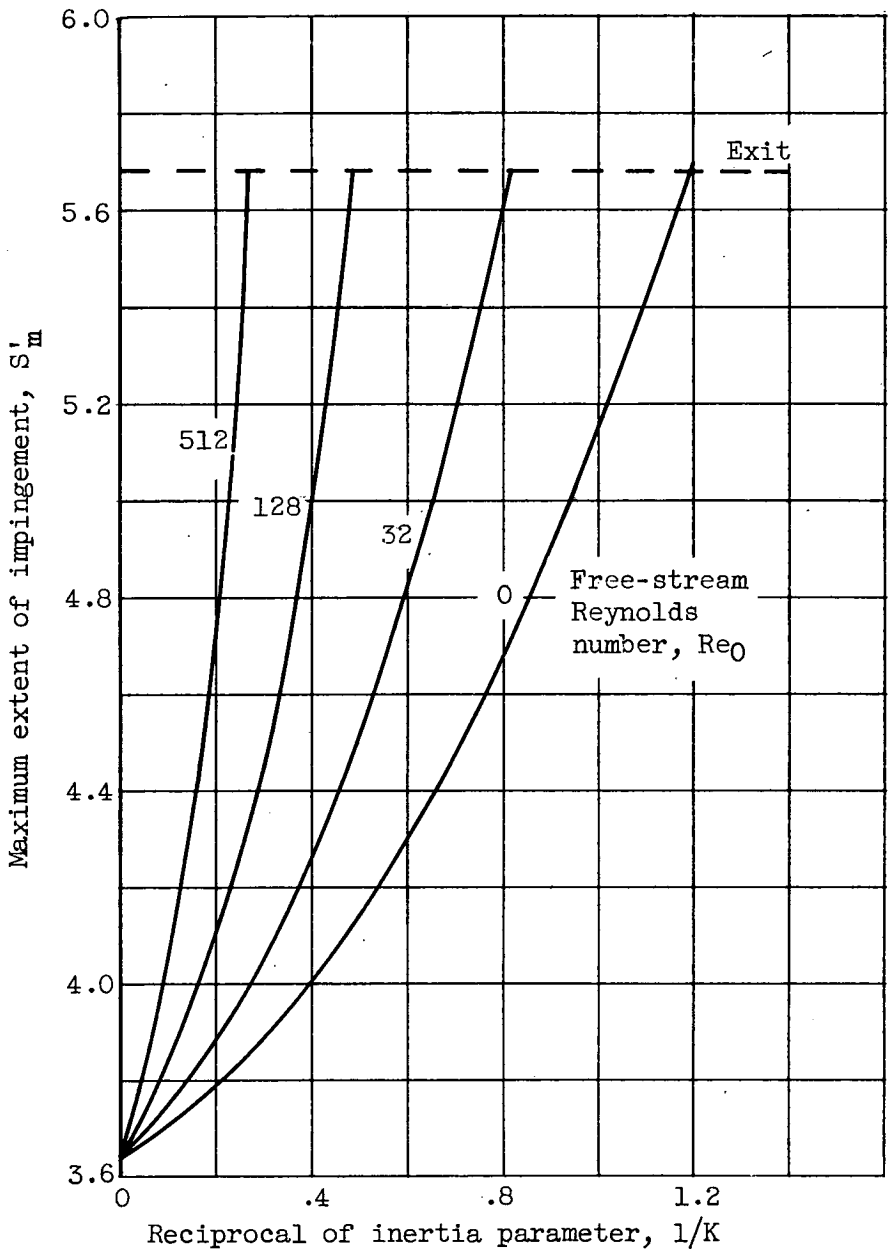

Figure 6. - Maximum extent of droplet impingement on outside wall of basic elbow as function of reciprocal of inertia parameter.

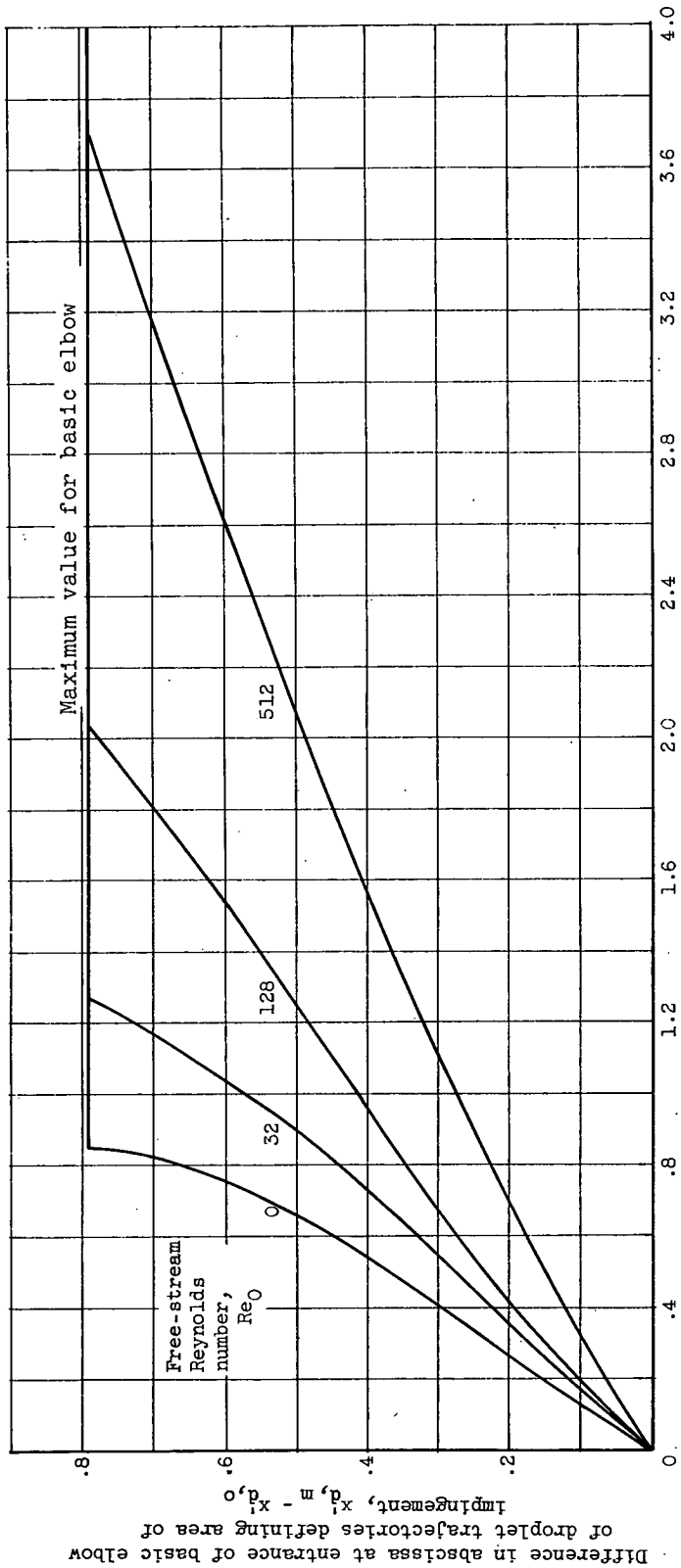

Figure 7. - Difference in abscissa at entrance of basic elbow of droplet trajectories defining area of impingement as function of inertia parameter.

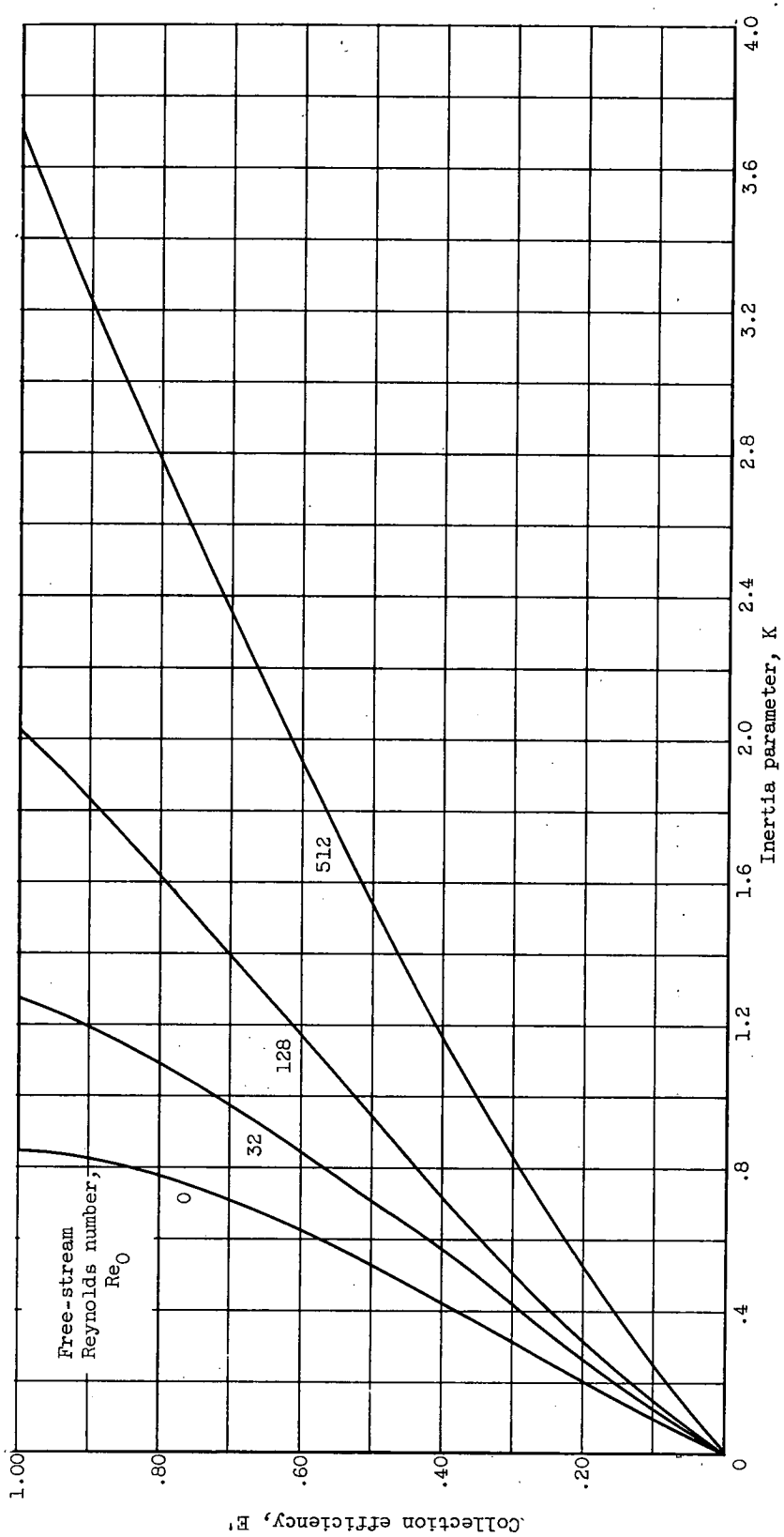

Figure 8. - Collection efficiency of basic elbow.

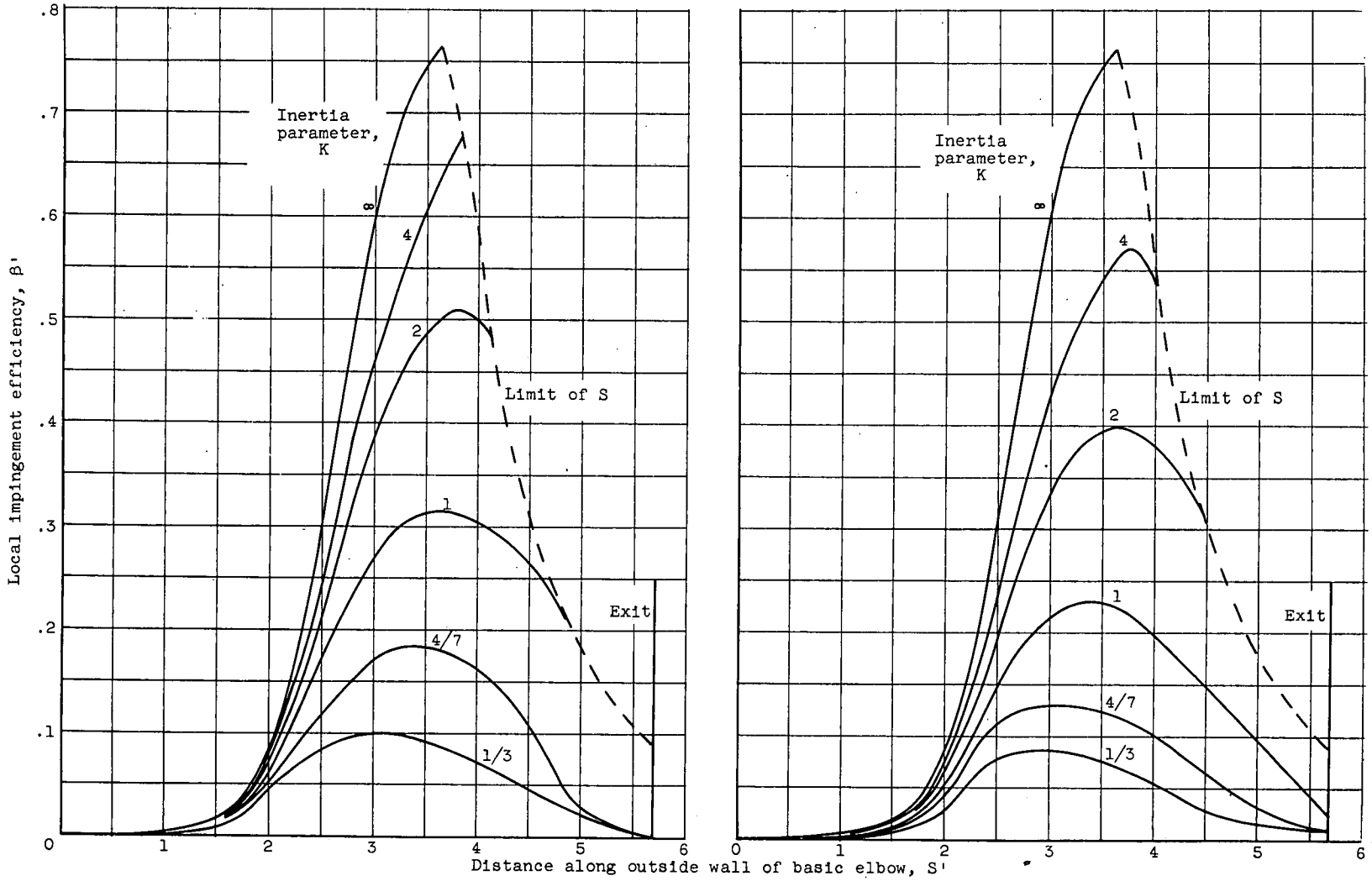

(a) Free-stream Reynolds number, 0.

(b) Free-stream Reynolds number, 32.

Figure 9. - Local impingement efficiency for basic elbow.

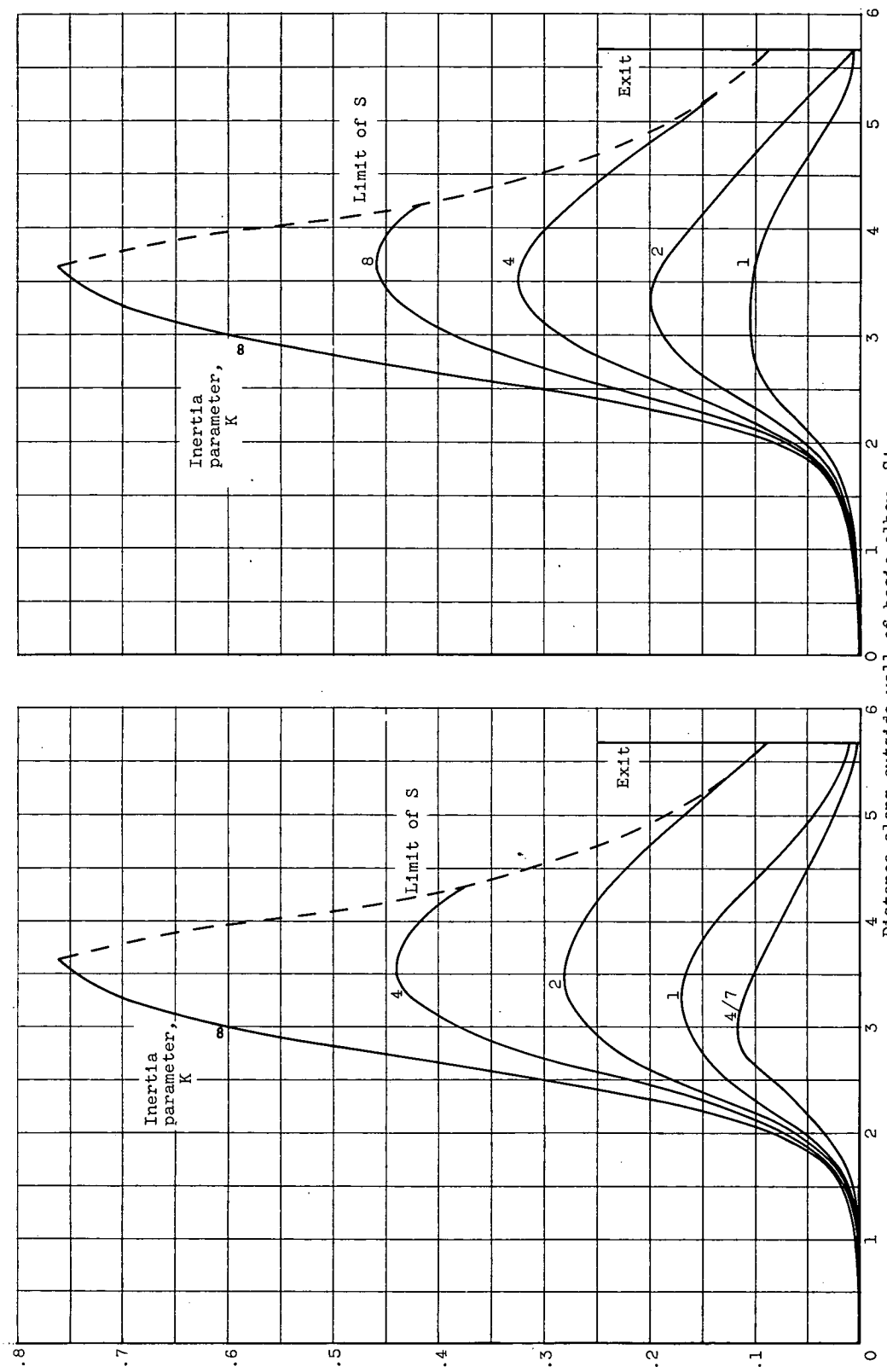

(c) Free-stream Reynolds number, 128.

(d) Free-stream Reynolds number, 512.

Figure 9. - Concluded. Local impingement efficiency for basic elbow.

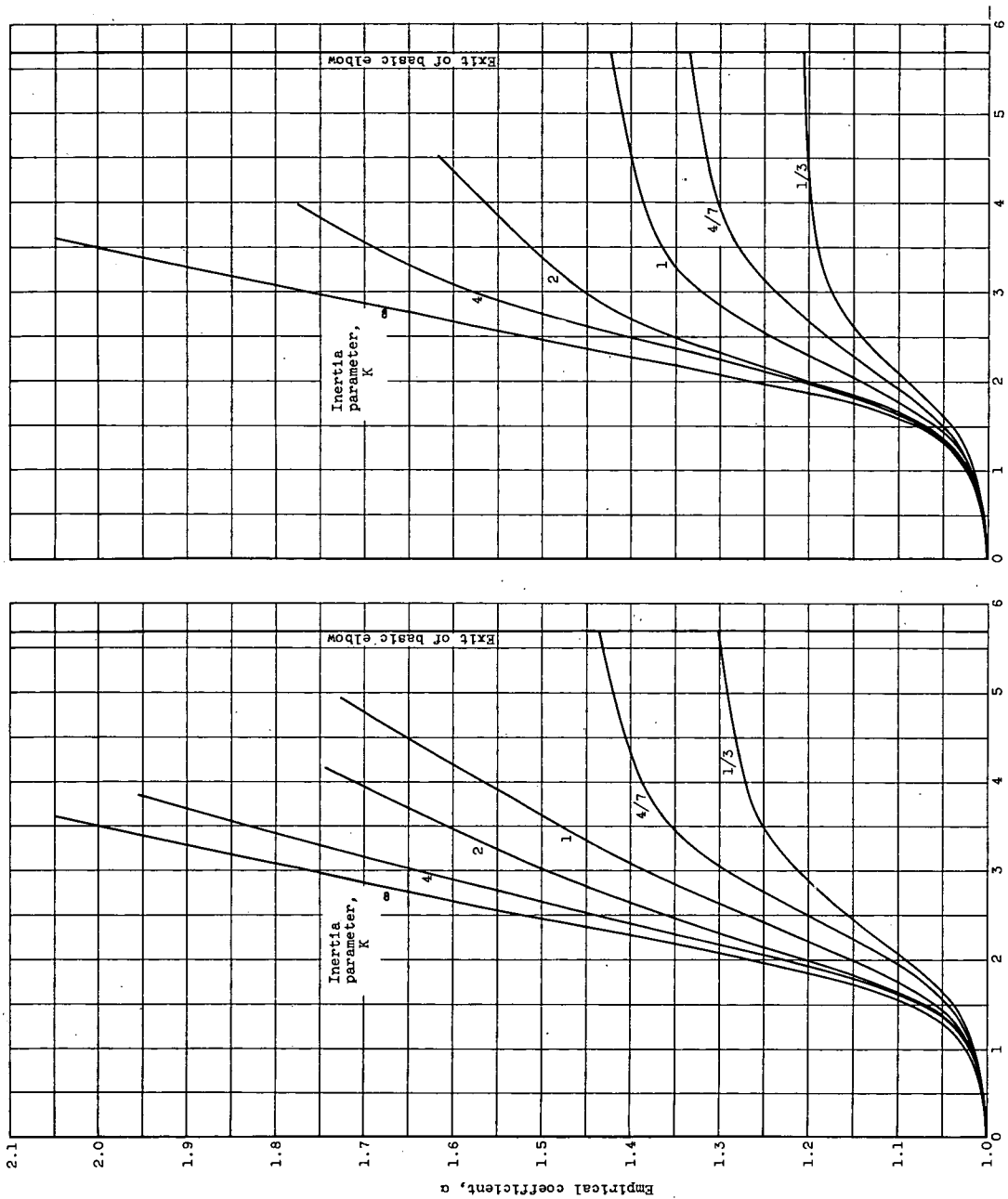

(a) Free-stream Reynolds number, 0.

(b) Free-stream Reynolds number, 32.

Figure 10. - Empirical coefficient α for equation (13) as function of distance along outside wall of supplementary elbow.

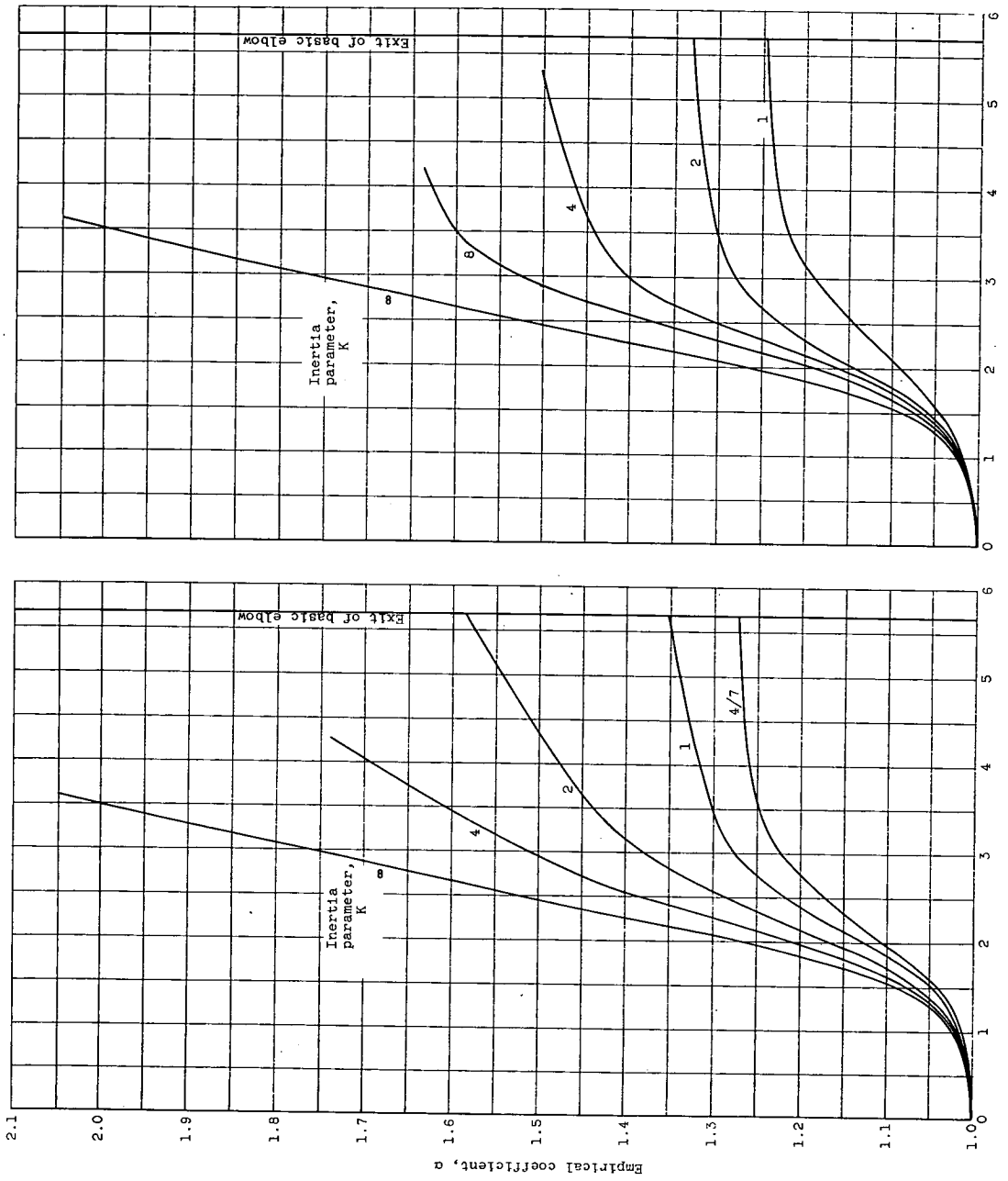

(c) Free-stream Reynolds number, 128.

(d) Free-stream Reynolds number, 512.

Figure 10. - Concluded. Empirical coefficient α for equation (13) as function of distance along outside wall of supplementary elbow.

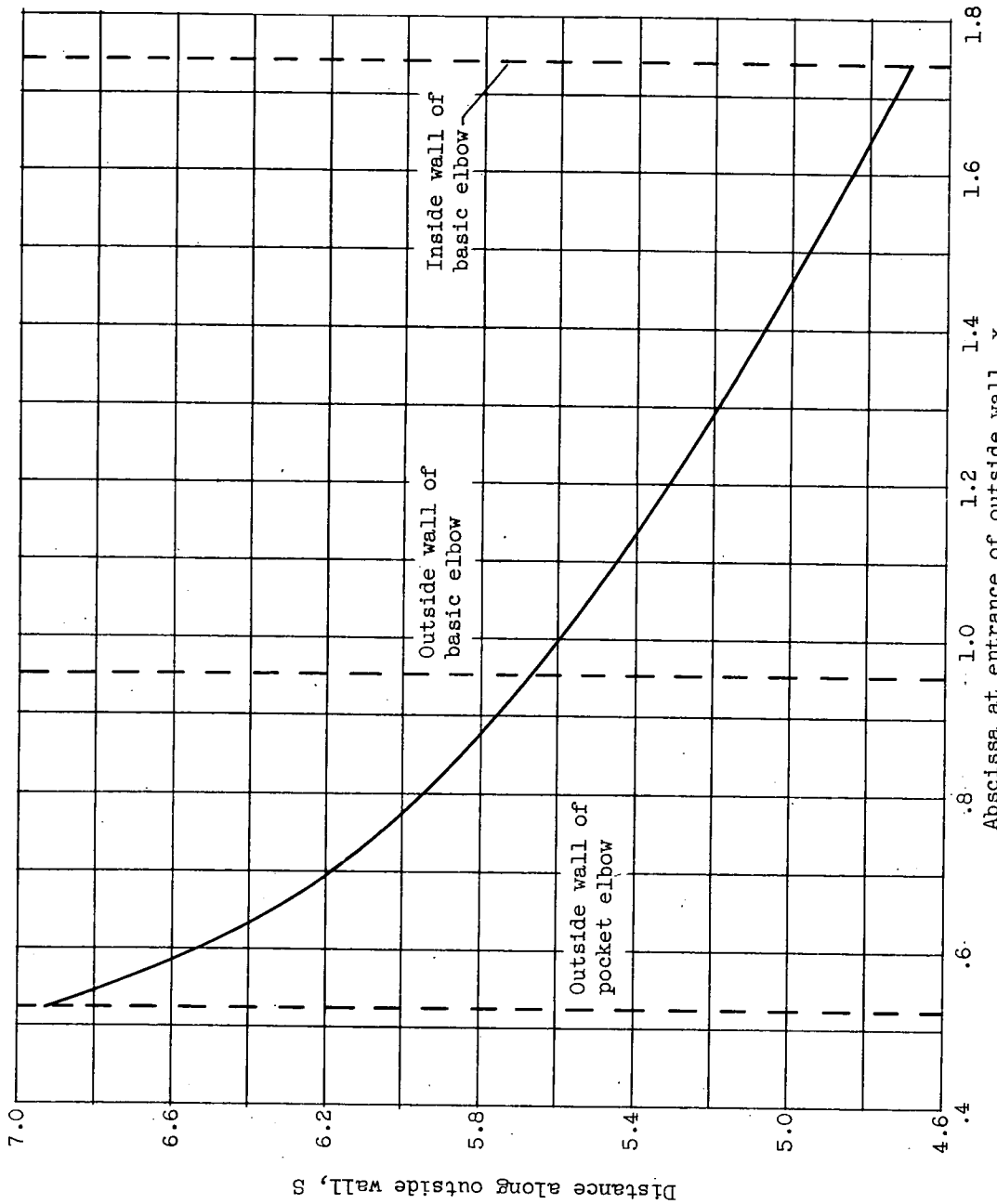

Figure 11. - Exit distance of outside wall of elbows as function of abscissa value of outside wall at entrance.

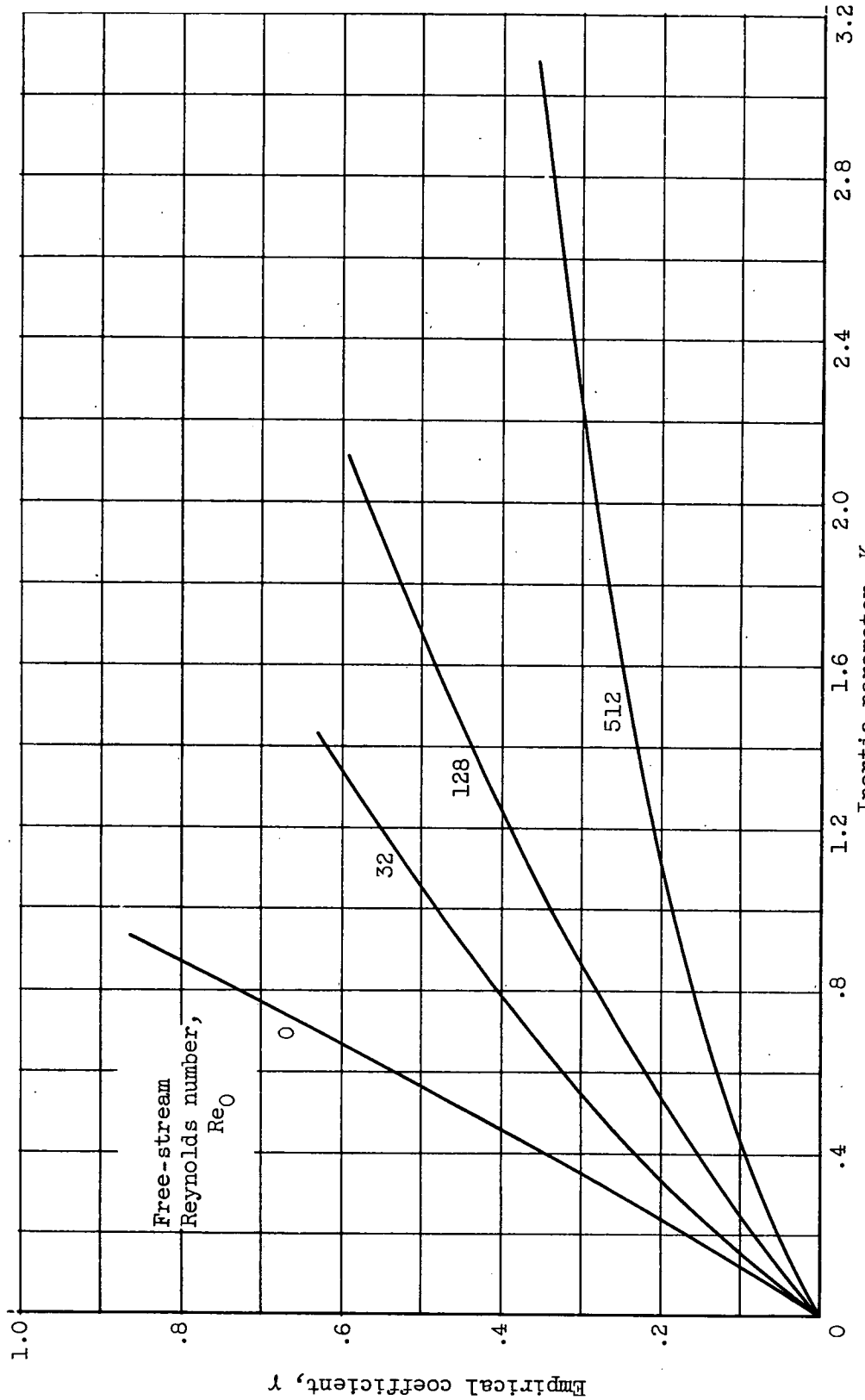

Figure 12. - Empirical coefficient γ for equation (15) as function of inertia parameter.

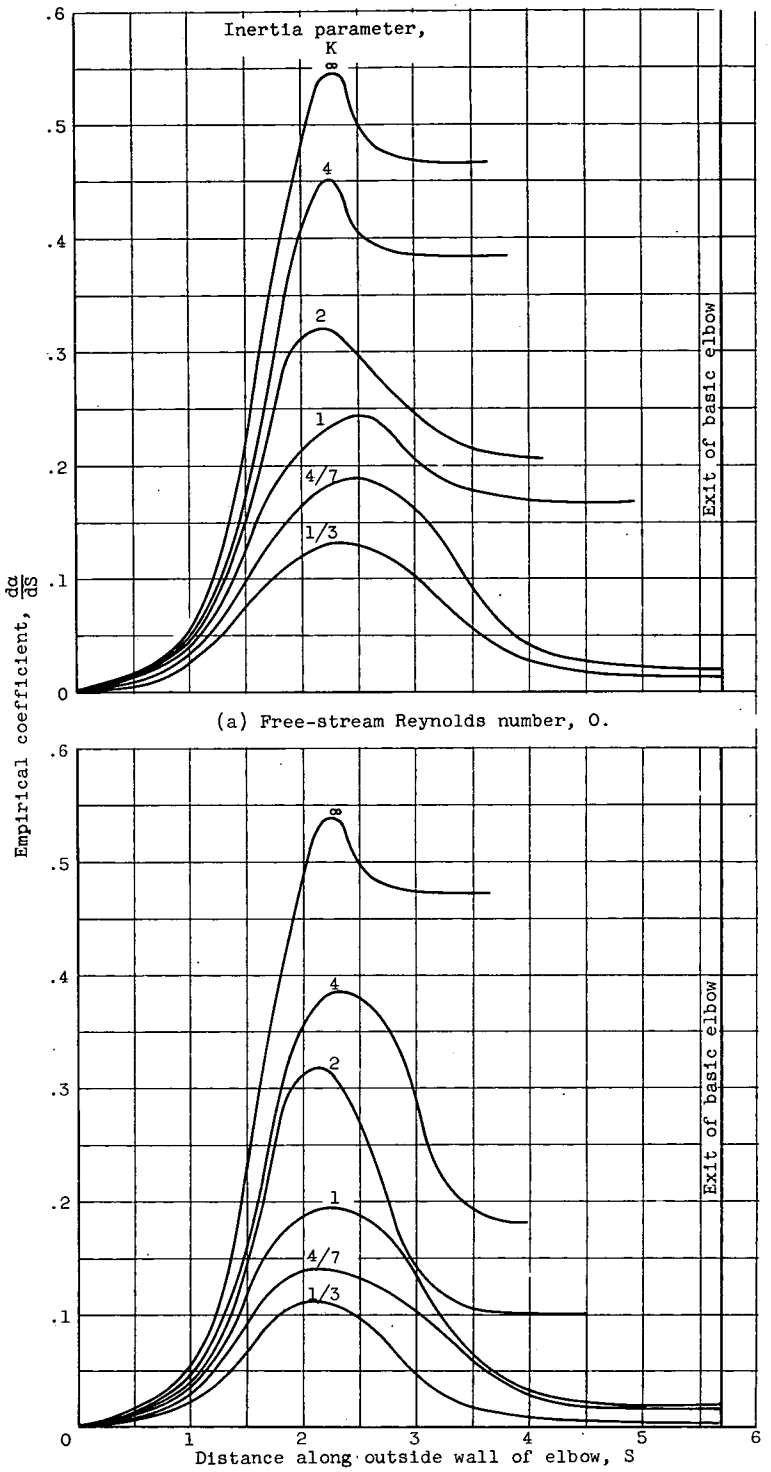

(a) Free-stream Reynolds number, 0.

(b) Free-stream Reynolds number, 32.

Figure 13. - Empirical coefficient $\frac{d\alpha}{dS}$ for equation (21) as function of distance along outside wall of supplementary elbow.

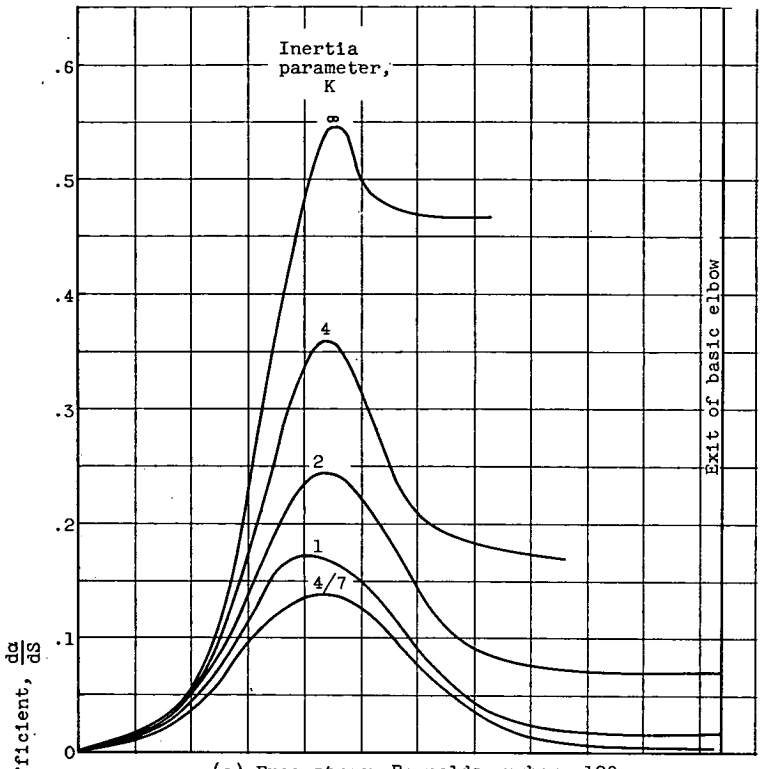

(c) Free-stream Reynolds number, 128.

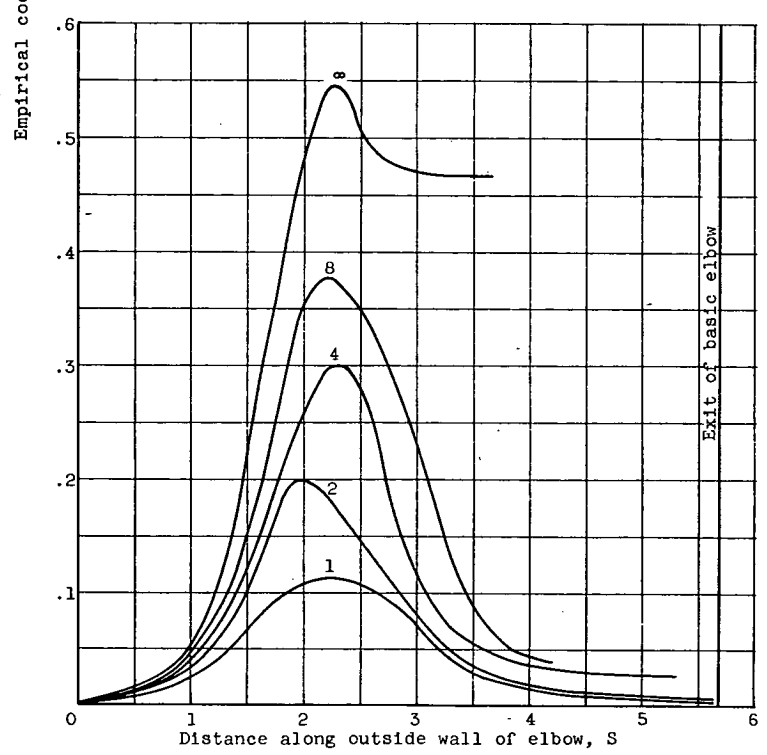

(d) Free-stream Reynolds number, 512.

Figure 13. - Concluded. Empirical coefficient $\frac{d\alpha}{dS}$ for equation (21) as function of distance along outside wall of supplementary elbow.

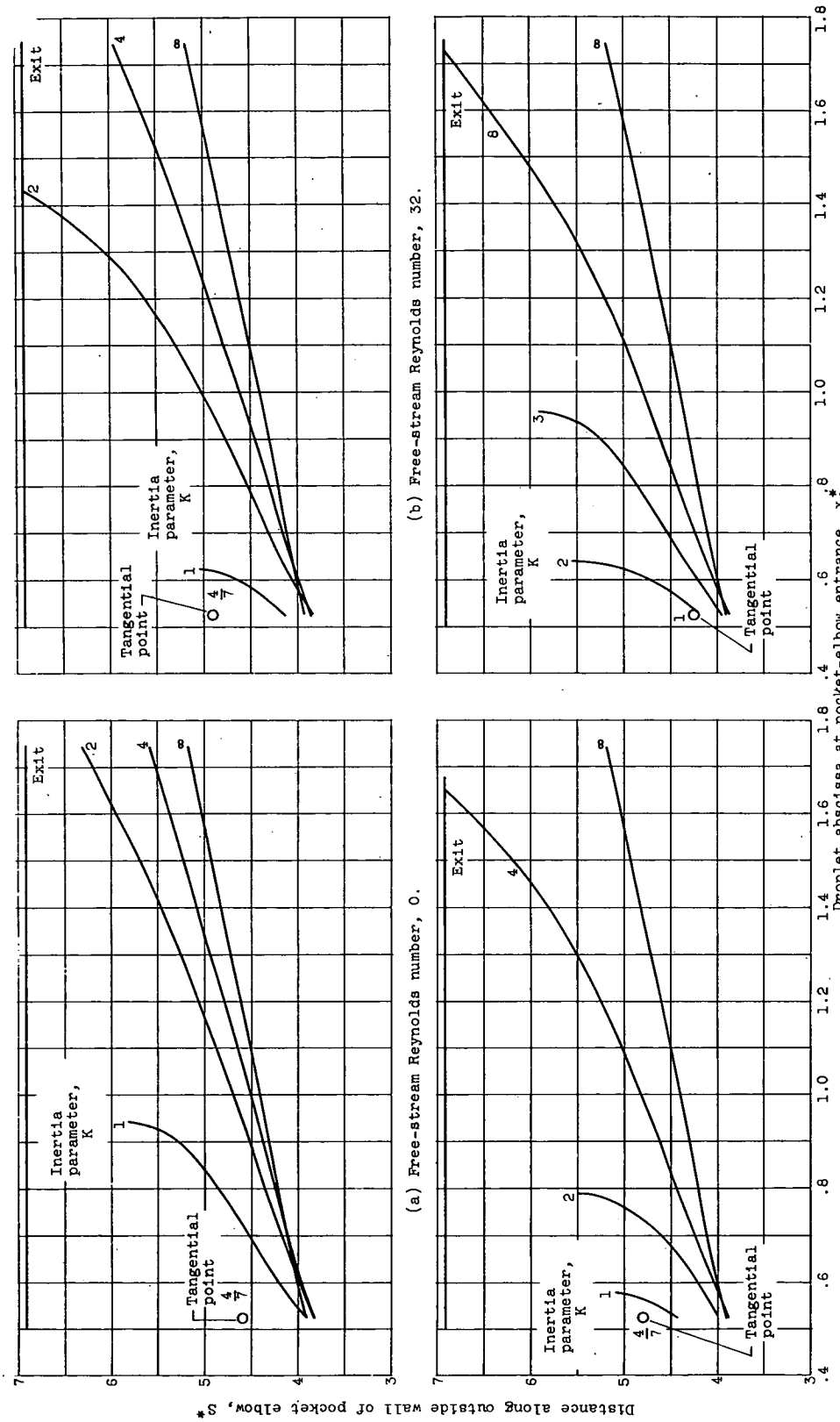

Figure 14. - Point of droplet impingement on outside wall of pocket elbow.

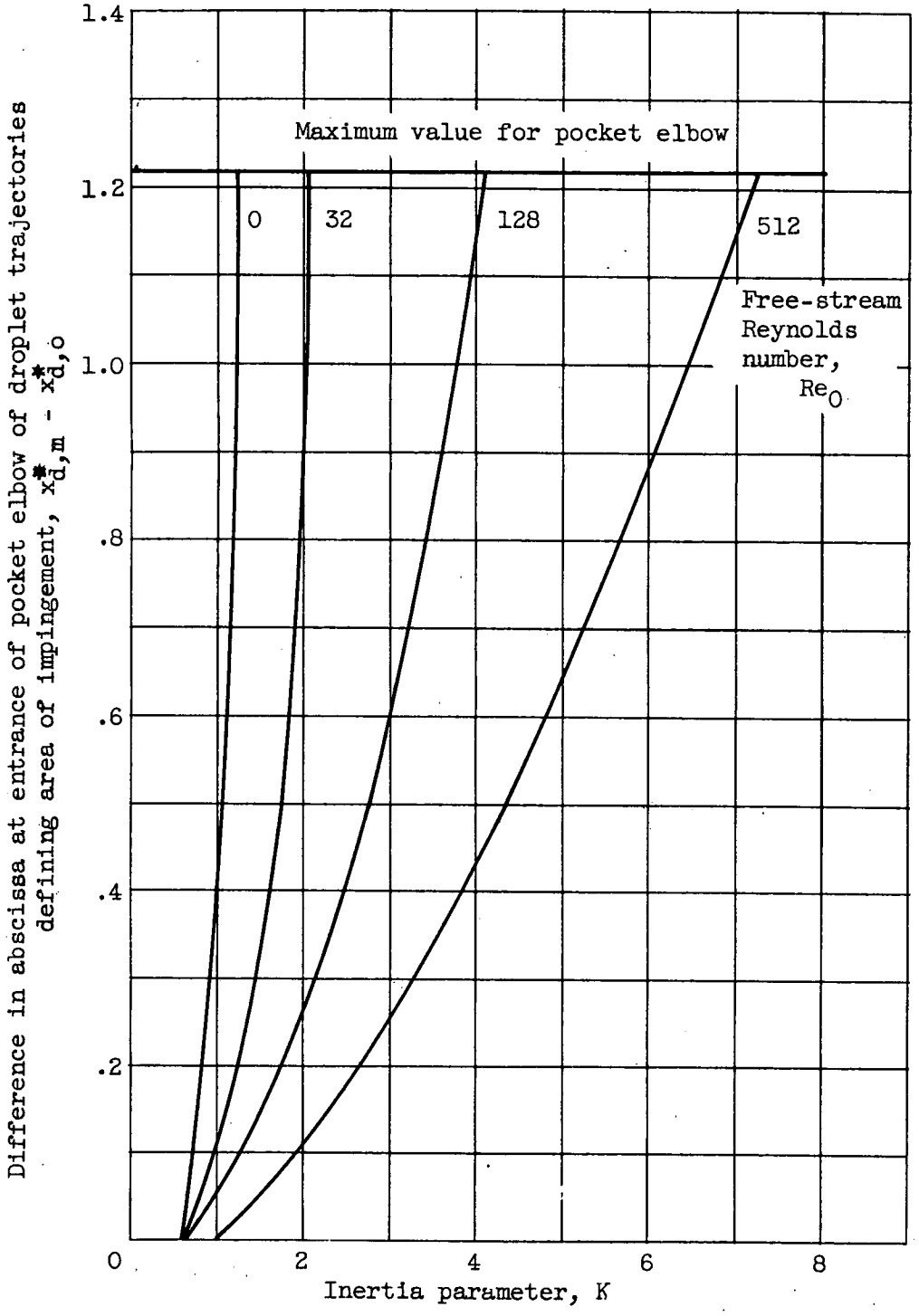

Figure 15. - Difference in abscissa values at entrance of pocket elbow of droplet trajectories defining area of impingement.

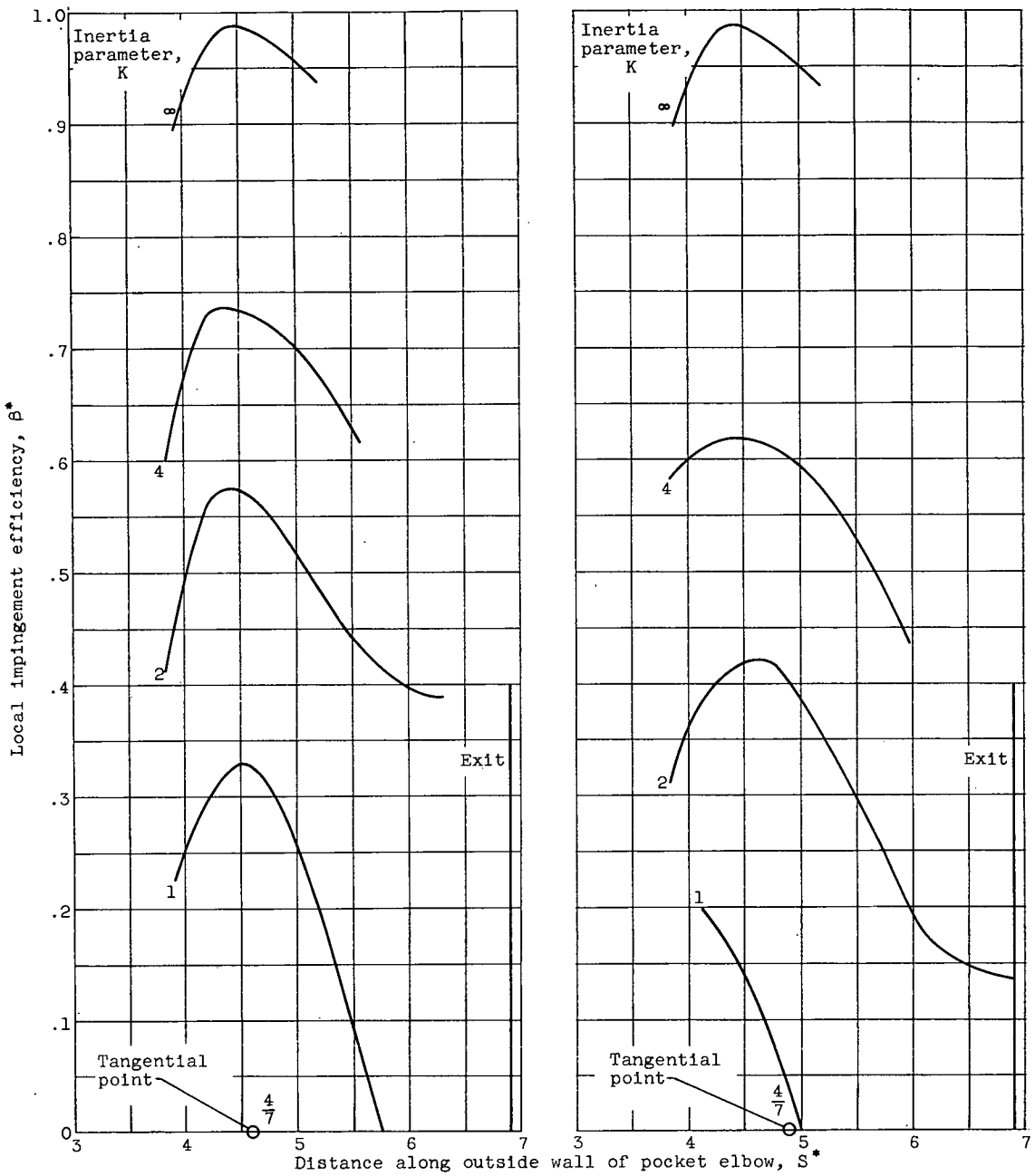

(a) Free-stream Reynolds number, 0. (b) Free-stream Reynolds number, 32.

Figure 16. - Local impingement efficiency for pocket elbow.

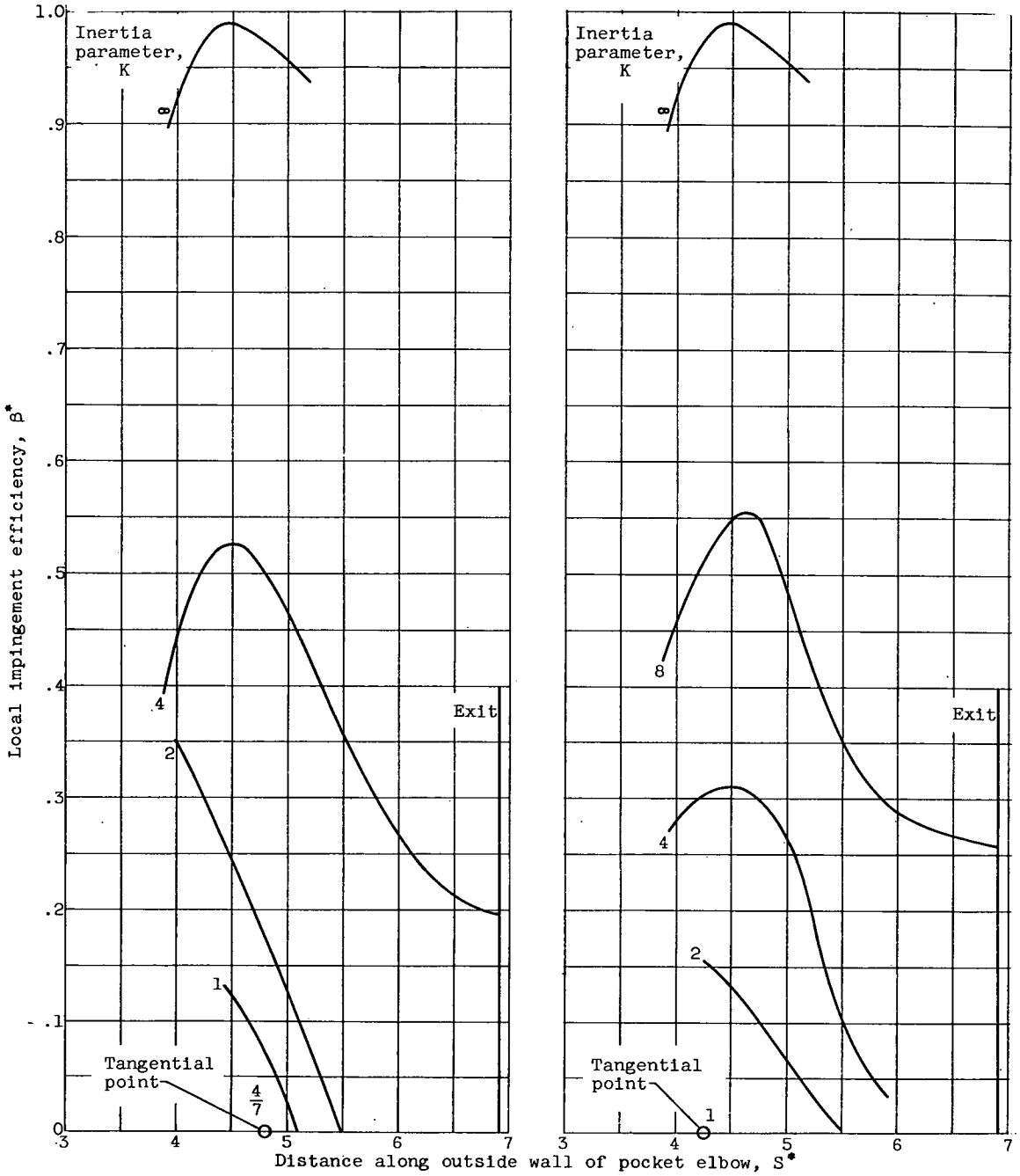

(c) Free-stream Reynolds number, 128. (d) Free-stream Reynolds number, 512.

Figure 16. - Concluded. Local impingement efficiency for pocket elbow.